Published in final edited form as:

J Nat Prod. 2017 March 24; 80(3): 648–658. doi:10.1021/acs.jnatprod.6b00924.

Cardiac Glycoside Constituents of *Streblus asper* with Potential Antineoplastic Activity

Yulin Ren[†], **Wei-Lun Chen**[‡], **Daniel D. Lantvit**[‡], **Ellen J. Sass**[§], **Pratik Shriwas**[⊥,∥,∇], **Tran Ngoc Ninh**[○], **Hee-Byung Chai**[†], **Xiaoli Zhang**[Δ], **Djaja D. Soejarto**[⊤,‡], **Xiaozhuo Chen**[⊥,∥,∇,⋕], **David M. Lucas**[†,§], **Steven M. Swanson**[‡,┤], **Joanna E. Burdette**[‡], and **A. Douglas Kinghorn**[†,*]

[†]Division of Medicinal Chemistry and Pharmacognosy, College of Pharmacy, The Ohio State University, Columbus, OH 43210, United States

[§]Division of Hematology, Department of Internal Medicine, College of Medicine, The Ohio State University, Columbus, OH 43210, United States

[Δ]Center for Biostatistics, The Ohio State University, Columbus, OH 43210, United States

[‡]Department of Medicinal Chemistry and Pharmacognosy, College of Pharmacy, University of Illinois at Chicago, Chicago, IL 60612, United States

[⊥]Department of Biological Sciences, Ohio University, Athens, OH 45701, United States

[∥]Edison Biotechnology Institute, Ohio University, Athens, OH 45701, United States

[∇]Molecular and Cellular Biology Program, Ohio University, Athens, OH 45701, United States

[⋕]Department of Biomedical Sciences, Ohio University, Athens, OH 45701, United States

[○]Institute of Ecology and Biological Resources, Vietnam Academy of Science and Technology, Hoang Quoc Viet, Cau Giay, Hanoi, Vietnam

[⊤]Science and Education, Field Museum of Natural History, Chicago, IL 60605, United States

[┤] School of Pharmacy, University of Wisconsin-Madison, Madison, WI 53705, United States

Abstract

[*]**Corresponding Author**. kinghorn.4@osu.edu.

DEDICATION

Dedicated to Professor Phil Crews, of the University of California, Santa Cruz, for his pioneering work on bioactive natural products.

ASSOCIATED CONTENT

Supporting Information.

The Supporting Information is available free of charge on the ACS Publications website at DOI: 10.1021/acschembio.5b01018.

Mass and NMR spectra of compounds **1**–**5** and **5a**–**5g**; ECD and UV spectra of compounds **5a**–**5g**; schemes of synthesis of **5a**–**5g** from **5**; diagrams of COSY, the key HMBC, and selective NOESY correlations of compounds **2**–**5** and **5a**–**5g**; in vivo data of **5** against MDA-MB-435 ells; assignments of the ^{1}H and ^{13}C NMR data of the known compounds **4** and **5a** and the synthetic derivatives **5a**–**5g**; and analytical data of the known compounds **4** and **5**.

ORCID

A. Douglas Kinghorn: 0000-0002-6647-8707

The authors declare no competing financial interest.

Three new (**1–3**) and two known (**4** and **5**) cytotoxic cardiac glycosides were isolated and characterized from a medicinal plant, *Streblus asper*, collected in Vietnam, with six new and one known derivatives (**5a–5g**) synthesized from (+)-strebloside (**5**). A preliminary structure-activity relationship study indicated that the C-19 formyl and C-5 and C-14 hydroxy groups and C-3 sugar unit play important roles in the mediation of the cytotoxicity of (+)-strebloside (**5**) against HT-29 human colon cancer cells. When evaluated in NCr *nu/nu* mice implanted intraperitoneally with hollow fibers facilitated with either MDA-MB-231 human breast or OVCAR3 human ovarian cancer cells, (+)-strebloside (**5**) showed significant cell growth inhibitory activity in both cases, in the dose range 5–30 mg/kg.

Graphical abstract

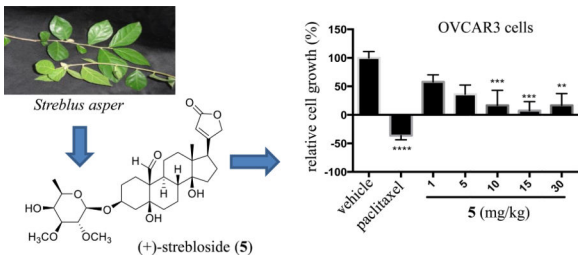

Moraceae (the mulberry or fig family) is a group of flowering plants comprising about 40 genera that have over 1000 species distributed in tropical and subtropical regions, of which the genus *Streblus* contains about 25 species.[1] One of these is *Streblus asper* Lour., known as the “toothbrush tree”, with various parts having been used in the Ayurvedic medicinal system.[2] When Swiss albino mice inoculated by Dalton’s ascitic lymphoma cells were treated with an ethyl acetate extract of the bark of *S. asper* (i.p., 200 or 400 mg/kg for nine consecutive days), the tumor volume was found to be decreased, with the survival parameters of mice increased.[2] Several cardiac glycosides have been characterized from *S. asper*,[3–6] and (+)-strebloside (**5**), occurring in high abundance, has been characterized as the main cytotoxic component.[5]

Many cardiac glycosides have been reported to show potent cytotoxicity toward different human cancer cell lines.[7,8] For example, digoxin, isolated originally from *Digitalis lanata* Ehrh. (Plantaginaceae)[9,10] and used traditionally to treat congestive heart failure,[11] was found to exhibit anticancer potential.[12] It inhibited neuroblastoma growth in vitro and in vivo[13] and has emerged as a potential anticancer lead for the treatment of prostate cancer.[14] Recently, a phase II clinical trial for the treatment of recurrent prostate cancer has been completed for digoxin.[15] Oleandrin, the cardiac glycoside main component of a standardized *Nerium oleander* plant-based botanical drug, Anvirzel™, has been developed as a potential cancer chemotherapeutic agent.[7,16]

In a continuing search for anticancer agents from higher plants,[17] a chloroform-soluble extract of the stem bark of *S. asper* collected in Vietnam was found to be highly cytotoxic toward the HT-29 human colon cancer cell line. Fractionation guided by bioassay against this cell line yielded three new (**1–3**) and two known (**4** and **5**) cardiac glycosides from this plant. Also, six new analogues and a known derivative were synthesized from (+)-strebloside

(**5**). All compounds were tested for their cytotoxicity toward the HT-29 cell line, and **5** was further evaluated for its growth inhibitory activity against a small panel of human cancer and normal human cell lines, and for its in vivo antitumor efficacy, using a hollow fiber test system.

RESULTS AND DISCUSSION

A sample of the stem bark of *S. asper* collected in Vietnam was extracted with MeOH, and the extract was partitioned with *n*-hexane and $CHCl_3$. When the cytotoxic $CHCl_3$ partition was subjected to chromatographic separation guided by inhibitory activity against the HT-29 cell line, three new cardiac glycosides, (+)-19-hydroxykamaloside (**1**), (+)-5-hydroxyasperoside (**2**), and (+)-3'-de-*O*-methylkamaloside (**3**), and two known analogues, (+)-3-*O*-*β*-D-fucopyranosylperiplogenin (**4**)[18] and (+)-strebloside (**5**)[5] were isolated.

Compound **1** was purified as an amorphous colorless powder with a molecular formula of $C_{31}H_{48}O_{10}$, as shown by a sodiated molecular ion peak at *m/z* 603.3153 (calcd 603.3140) observed in the HRESIMS, in conjunction with the ^1H and ^{13}C NMR spectroscopic data (Tables 1 and 2). The UV (λ_{max} 216 nm) and IR (ν_{max} 3459, 1743 and 1621 cm^{-1}) spectra showed the absorptions of hydroxy groups and an unsaturated lactone unit.[19,20] The ^1H and ^{13}C NMR data of **1** (Tables 1 and 2)[21] exhibited the characteristic resonances for a cardiac glycoside, including two methyl groups, a sugar moiety, and a lactone unit.[19,20] Comparison of the ^{13}C NMR data of **1** with those of (+)-strebloside (**5**)[5] showed that the resonance for C-19 of **5** at δ_C 208.3 was replaced by that at δ_C 65.0 in **1** (Table 2). The resonances for C-5 and C-10 of **5** were different from those for these carbons of **1**, but they were closely comparable for other carbons of both compounds. Thus, compound **1** could be defined as 19-nor-10-hydroxymethylstrebloside, an analogue of digoxin.

The conformation of the cardenolide ring system of digoxin has been proposed previously by investigation of its NMR spectroscopic parameters,[22] and this was confirmed by that generated by a *Mercury* program,[23] based on the reported crystal structure of digoxin (Figure 1).[10] Using Snatzke's method, the ECD spectrum induced by $[Mo_2(OAc)_4]$ of digoxin showed a positive Cotton effect (CE) at 310 nm and a positive O-C-C-O dihedral angle (Figure 2), which indicated a (3'c*S*, 4'c*S*) absolute configuration.[24] Thus, a (3*S*, 5*R*, 8*R*, 9*S*, 10*S*, 12*R*, 13*S*, 14*S*, 17*R*, 1'a*R*, 3'a*S*, 4'a*S*, 5'a*R*, 1'b*S*, 3'b*S*, 4'b*S*, 5'b*R*, 1'c*S*, 3'c*S*, 4'c*S*, 5'c*R*) absolute configuration was confirmed for digoxin from its induced ECD data and previously published crystal structure. A positive CE at 239 nm observed in the ECD spectrum of digoxin (Figure 3) correlated to a 17*R* configuration. This same configuration could be assigned for **1** from its ECD spectrum, which was consistent with that of digoxin (Figure 3). This determination was also supported by the resonances for H-17 and C-18 of **1**, which were consistent with those reported for a cardiac glycoside comprising a 17β-lactone unit but different from those published for a 17-*epi*-cardiac glycoside containing a 17α-lactone unit.[25] These changes would result from the stereoelectronic effects of the C-17 lactone unit, the same as those reported for bicyclic alcohols.[26]

Conformational effects have been also observed for other protons and carbons of cardenolides. For example, the chemical shift of C-4 at δ_C 41.3 of a 3α-hydroxycardenolide

appeared at δ_C 36.9 in its 3-epimer.[27] Also, the NMR resonances for H-7/C-7 at δ_H 2.0/δ_C 28.0 and H-9/C-9 at δ_H 0.9/δ_C 50.0 in a 5α*H*-cardenolide shifted to those at δ_H 1.5/δ_C 22.0 for H-7/C-7 and at δ_H 1.7/δ_C 35.0 for H-9/C-9 in its 5-epimer.[28] Following these observations, the resonances for C-4 at δ_C 34.9, C-7/H-7 at δ_C 19.0/δ_H 1.39 and 2.59, and C-9/H-9 at δ_C 39.1/δ_H 1.57 (Table 2) of **1** supported the presence of 3-*O*-β-glycosyl and 5β-hydroxy groups.[27–29] The occurrence of the same conformation for the cardenolide core of **1** as that for digoxin was also confirmed by the NOESY correlations between H-3 and H-7α, H-7α and H-9, OH-5 and H-8, H-8 and H-18, and H-18 and H-19 of **1** (Figure 1).

Owing to the overlapped signals observed for H-1'–H-3' and H-5' of **1**, determination of the relative configuration of the sugar unit proved to be difficult. Fortunately, this problem was resolved when acetone-d_6 rather than $CDCl_3$ was employed as the NMR solvent (Table 1). The NOESY correlations observed between H-1' and H-9, H-3', H-5', and OCH_3-2', and between OH-4' and OH-5, OH-19, and H-6' (Figure 1), indicated that H-1', H-3', H-4', and H-5' are α-oriented, and H-2' and H-6' are β-oriented. Therefore, a (3*S*, 5*S*, 8*R*, 9*S*, 10*R*, 13*R*, 14*S*, 17*R*, 1'*R*, 2'*R*, 3'*S*, 4'*S*, 5'*R*) absolute configuration could be assigned for **1** [(+)-19-hydroxykamaloside], with the structure determined as (3β,5β)-3-[(2,3-di-*O*-methyl-β-D-fucopyranosyl)oxy]-5,14,19-trihydroxycard-20(22)-enolide.

Compound **2** was isolated as an amorphous colorless powder. The similar UV and IR spectra to those of **1** indicated that **2** is also a cardiac glycoside. The same molecular formula of **2** [positive-ion HRESIMS *m/z* 603.3152 (calcd for $C_{31}H_{48}O_{10}Na$, 603.3140), as observed in the HRESIMS] to that of **1** showed these compounds to be regioisomers. Comparison of their ^1H and ^{13}C NMR spectroscopic data (Tables 1 and 2) suggested that both compounds contain a 5,14-dihydroxycardenolide core substituted with a 2',3'-*di*-*O*-methylglycose unit at C-3. The 19-hydroxymethyl and 6'-methyl groups of **1** were substituted by a 19-methyl group and a 6'-hydroxymethyl group in **2**, as supported by the HMBC cross-peaks observed between H-19 and C-1 and C-9, H-6' and C-4', and H-3' and C-6' for **2** (Figure S14, Supporting Information).

A 17*R* absolute configuration could be defined for **2** from the positive CE at 236 nm observed in its ECD spectrum, consistent with that of **1**, and this was supported by the resonances for H-17 at δ_H 2.81 and C-18 at δ_C 15.7, which were indicative of a 17β-lactone unit.[25] A 3-*O*-β-glycosyl moiety and a 5β-hydroxy group were evident in **2** due to the resonances for C-4 at δ_C 34.2, C-7/H-7 at δ_C 23.8/δ_H 1.17 and 1.89, and C-9/H-9 at δ_C 39.2/δ_H 1.51 (Table 2).[27–29] These were confirmed by the NOESY correlations observed between H-3 and H-7α, H-7α and H-9, H-8 and H-19, and H-18 and H-19 (Figure S15, Supporting Information). Thus, the same conformation and relative configuration of the cardenolide moiety of **1** occurred in **2**. The NOESY correlations observed between H-1' and H-3, H-3', and H-5', and between H-4' and H-2' and H-6' (Figure S15, Supporting Information), indicated an α-orientation for H-1', H-3', H-5' and a β-orientation for H-2', H-4', and H-6'. These assignments were supported by the resonances for C-1'–C-6' of **2**, which were closely comparable with those of asperoside.[6] Thus, a (3*S*, 5*S*, 8*R*, 9*S*, 10*R*, 13*R*, 14*S*, 17*R*, 1'*R*, 2'*R*, 3'*S*, 4'*R*, 5'*R*) absolute configuration could be defined for **2** [(+)-5-hydroxyasperoside], with its structure characterized therefore as (3β,5β)-3-[(2,3-di-*O*-methyl-β-D-glucopyranosyl)oxy]-5,14-dihydroxycard-20(22)-enolide.

Compound **3** was isolated as an amorphous colorless powder. The similar UV, IR, and NMR spectra with those of **1** and **2** indicated that **3** is a further cardiac glycoside. The molecular formula determined from the positive-ion HRESIMS *m/z* 573.3054 (calcd for $C_{30}H_{46}O_9Na$, 573.3034) indicated an OCH_2 unit to be missing from **3**, when compared with either **1** or **2**, as confirmed by the NMR resonances for a single methoxy group at δ_H 3.38 s and δ_C 57.1 observed for **3** (Tables 1 and 2). Comparison of the ^1H and ^{13}C NMR spectroscopic data of **3** with those of the known compound **4** (Tables 1 and 2 and Table S1, Supporting Information) indicated that both compounds possess the same cardenolide aglycone but a different sugar unit. A methoxy group was proposed at C-2' of **3**, as indicated by the HMBC cross-peak observed between the methoxy group and C-2'. The 17*R* absolute configuration could be defined for **3** from a positive CE at 241 nm in the ECD spectrum, which was consistent with **1** and **2**. The same conformation as that of **2** for its cardenolide unit was evident for **3**, from the closely comparable NMR resonances for this moiety of **2** and **3**. A (3*S*, 5*S*, 8*R*, 9*S*, 10*R*, 13*R*, 14*S*, 17*R*, 1'*R*, 2'*R*, 3'*S*, 4'*R*, 5'*R*) absolute configuration was characterized for **3** from the NOESY correlations observed between H-3 and H-7α and H-17, H-7α and H-9, H-8 and H-18 and H-19, H-18 and H-22, H-1' and H-3, H-3', H-4', and H-5', and between OH-4' and H-6' (Figure S15, Supporting Information). Therefore, compound **3** was assigned structurally as (3β,5β)-3-[(2-*O*-methyl-β-D-fucopyranosyl)oxy]-5,14-dihydroxycard-20(22)-enolide, and has been accorded the trivial name, (+)-3'-de-*O*-methylkamaloside.

The structures of the two known cardiac glycosides **4** and **5** isolated from the stem bark of *S. asper* in the present study were determined by comparison of their spectroscopic data (Tables 1 and 2 and Table S1, Supporting Information) with literature data for (+)-3-*O*-β-D-fucopyranosylperiplogenin (**4**)[18] and (+)-strebloside (**5**),[5] respectively. The (3*S*, 5*S*, 8*R*, 9*S*, 10*R*, 13*R*, 14*S*, 17*R*, 1'*R*, 2'*R*, 3'*S*, 4'*R*, 5'*R*) and (3*S*, 5*S*, 8*R*, 9*S*, 10*S*, 13*R*, 14*S*, 17*R*, 1'*R*, 2'*R*, 3'*S*, 4'*S*, 5'*R*) absolute configurations were evident for **4** and **5**, respectively, from their ECD and 2D NOESY NMR spectra, which were consistent with those of **1** (Figures 1 and 3 and Figures S15 and S16, Supporting Information).

Compounds **1–5**, along with a commercially available sample of digoxin, were evaluated for their cytotoxicity against the HT-29 human colon cancer cell line, using paclitaxel as the positive control (Table 3).[30] The compounds obtained in sufficient quantity were also tested for their activity toward the human MV4–11 and Kasumi-1 leukemia cell lines[31] and the H1299 human non-small cell lung cancer cell line,[32] using silvestrol and paclitaxel as the positive controls, respectively (Table 3). All compounds tested showed potent cytotoxicity that was comparable with digoxin, with IC_{50} values in the range 93–690 nM (Table 3), indicating that they are the cytotoxic principles of the stem bark of *S. asper*. Interestingly, both compounds **1** and **4** showed more potent activity than paclitaxel toward H1299 cells (Table 3).

The major active compound, (+)-strebloside (**5**), and digoxin were also tested for their selectivity, using normal human CCD-112CoN colon, NL20 lung, and peripheral blood mononuclear cells.[31–33] The potency of both agents toward normal human cells was found to be much lower than that against human cancer cells, indicating that both **5** and digoxin showed selective cytotoxicity toward human colon and lung cancer and leukemia cells. The

selectivity of **5** observed toward HT-29 cells and CCD-112CoN cells was greater than digoxin (Tables 3 and 4).

To characterize the functional groups that were responsible for the cytotoxicity of (+)-strebloside (**5**), several derivatives (Figure 4) were synthesized from **5** (Scheme 1 and Schemes S1–S4, Supporting Information), which was isolated in a relatively large quantity from *S. asper* with a yield of 0.15‰ w/w. The synthesized compounds were defined structurally through comparison of their spectroscopic data with those of **5** (Tables 1 and 2 and Tables S1–S4, Supporting Information) and evaluated by their cytotoxicity against the HT-29 cell line (Table 5).[30]

Previously, the cytotoxic potency of a lignan lactone was found to be increased by acetylation of its saccharide unit,[33] and the presence of different glycosyl units of cardiac glycosides contributed diversely to the cytotoxicity of these compounds, as exemplified by **2** (IC_{50} 690 nM) and **4** (IC_{50} 90 nM) (Table 3). Thus, acetylation was included as the first step in the investigation of the structure-cytotoxicity relationship of **5**.

When **5** was treated with Ac_2O and pyridine, (+)-4'-*O*-acetylstrebloside (**5a**) was produced. This product showed a sodiated molecular ion peak at *m/z* 643.3109 for a molecular formula of $C_{33}H_{48}O_{11}Na$ and the NMR resonances for a C-4' acetyl group (Table S1, Supporting Information), as indicated by the HMBC cross-peak between H-4' and the acetyl carbonyl group (Figure S14, Supporting Information). A (3*S*, 5*S*, 8*R*, 9*S*, 10*S*, 13*R*, 14*S*, 17*R*, 1'*R*, 2'*R*, 3'*S*, 4'*S*, 5'*R*) absolute configuration was defined for **5a** from its ECD and 2D NOESY NMR spectra, which were consistent with those of **5** (Figure 3 and Figures S15 and S16, Supporting Information).When tested against the HT-29 cell line, **5a** was slightly less active than **5** (Table 5).

To further test the importance of the C-4' substituent, several new benzoylated derivatives were prepared from **5**. When **5** was reacted with benzoyl chloride and pyridine, (+)-4'-*O*-benzoylstrebloside (**5b**) and (+)-4'-*O*-benzoyl-19-nor-kamaloside-10-carboxylic acid (**5c**) were obtained. The product **5b** showed a sodiated molecular ion peak at *m/z* 705.3260 for a molecular formula of $C_{38}H_{50}O_{11}$. It also exhibited the NMR resonances for an additional benzoyl group, when compared with those of **5** (Tables 1 and 2 and Tables S2 and S3, Supporting Information). The C-4' benzoyl group was implied by the HMBC between H-4' and the benzoyl carbonyl group (Figure S14, Supporting Information). A molecular formula of $C_{38}H_{50}O_{12}$, deduced for **5c** from its sodiated molecular ion peak at *m/z* 721.3214 (calcd 721.3194), indicated that this compound contains an additional oxygen atom, when compared with **5b**. A hydroxycarbonyl rather than a formyl group was defined at C-10 of **5c**, on account of the resonance for its C-19 at δ_C 176.1 rather than at δ_C 208.3 for the same carbon of **5b** (Table S3, Supporting Information). The product **5c** could be formed by the aerial oxidation of the C-10 formyl group of **5b**.

When **5** was treated with 4-chlorobenzoyl chloride, pyridine, and dichloromethane, (+)-4'-*O*-(4-chlorobenzoyl)strebloside (**5d**), (+)-4'-*O*-(4-chlorobenzoyl)-19-nor-kamaloside-10-carboxylic acid (**5e**), and (+)-4'-*O*-(4-chlorobenzoyl)-14(15)-anhydrostrebloside (**5f**) were obtained. Compound **5d** was defined structurally from its sodiated molecular ion peak at *m/z*

739.2862 for a molecular formula of $C_{38}H_{49}O_{11}Cl$ and the NMR resonances for an additional 4-chlorobenzoyl group, when compared with **5** (Tables 1 and 2 and Tables S2 and S3, Supporting Information). The 4-chlorobenzoyl group was shown to be at the C-4' position from the HMBC between H-4' and the benzoyl carbonyl group (Figure S14, Supporting Information). The product **5e** gave a sodiated molecular ion peak at *m/z* 755.2805 for a molecular formula of $C_{38}H_{49}O_{12}Cl$, 16 Da more than **5d**, indicating that **5e** contains an additional oxygen. A hydroxycarbonyl rather than a formyl group was linked at C-10 of **5e**, as indicated by the resonance for C-19 at δ_C 176.1 (Table S3, Supporting Information). Similar to the formation of **5c, 5e** might be generated from the aerial oxidation of **5d**. The product **5f** showed a sodiated molecular ion peak at *m/z* 721.2753 for a molecular formula of $C_{38}H_{47}O_{10}Cl$, 18 Da (H_2O) less than **5d**, indicating that **5f** is a dehydrated analogue of **5d**. This was verified by comparison of ^{13}C NMR spectroscopic data of **5f** with those of **5d**, in which the resonances for C-14 at δ_C 85.2 and C-15 at δ_C 32.0 of **5d** appeared at δ_C 152.7 for C-14 and δ_C 117.6 for C-15 of **5f** (Tables S3 and S4, Supporting Information).

The same (3*S*, 5*S*, 8*R*, 9*S*, 10*S*, 13*R*, 14*S*, 17*R*, 1'*R*, 2'*R*, 3'*S*, 4'*S*, 5'*R*) absolute configuration as determined for **5** was assigned for **5b–5e** from their consistent ECD and 2D NOESY NMR spectra. In turn, a (3*S*, 5*S*, 8*R*, 9*S*, 10*S*, 13*R*, 17*S*, 1'*R*, 2'*R*, 3'*S*, 4'*S*, 5'*R*) absolute configuration was defined for **5f**, from comparison of its ECD and 2D NOESY NMR spectra with those of **5** (Figure 3 and Figure S16, Supporting Information). Different from the ECD bands observed for **5** (Figure 3), a negative CE at 239 nm and a positive CE at 216 nm, indicative of a 17*S* configuration, occurred in the ECD spectrum of **5f** (Figure S16, Supporting Information). This probably resulted from the impact of the c/d-ring conformational change upon formation of the C-14/C-15 double bond, as evidenced previously.[34] When evaluated toward the HT-29 cell line,[30] **5b** and **5d** were cytotoxic, but **5c, 5e**, and **5f** were all inactive in this regard (Table 5).

To test the role of other substituents on mediating its cytotoxicity, (+)-strebloside (**5**) was subjected to acid hydrolysis. Treatment with trifluoroacetic acid (TFA) at 70 °C for 1 h afforded a new analogue, **5g**, with the C-19 formyl group transferred to the C-3 hydroxy group, which was purified from the reaction mixture. Compound **5g** showed a sodiated molecular ion peak at *m/z* 391.1899 for a molecular formula of $C_{23}H_{28}O_4$, with no resonances for a saccharide residue observed from its ^1H and ^{13}C NMR spectra, when compared with those of **5** (Tables 1, 2, and Table S4, Supporting Information). Three double bonds could be deduced from its ^{13}C NMR resonances, for C-5 at δ_C 125.0 and C-10 at δ_C 129.6, C-14 at δ_C 153.3 and C-15 at δ_C 116.0, and C-20 at δ_C 170.8 and C-22 at δ_C 116.5 (Table S4, Supporting Information). These assignments were supported by the HMBC observed between H-1 and C-5, H-2 and C-10, H-7 and C-14, H-15 and C-14 and C-17, and H-17 and C-22 (Figure S14, Supporting Information). A formate group indicated by a resonance at δ_C 161.2 (Table S4, Supporting Information) was assigned at the C-3 position, as implied by the HMBC between H-3 and the formate carbonyl group (Figure S14, Supporting Information). Thus, **5g** was characterized as (3β)-3-*O*-formyl-19-nor-card-5(10), 14(15),20(22)-trienolide or (+)-19-nor-5(10),14-dianhydrostrophanthidin-3-yl formate.

A 17*S* configuration was indicated for **5g** from its sequential negative and positive CEs at 242 and 213 nm in the ECD spectrum, which was consistent with that of **5f** (Figure S16, Supporting Information), and a (3*S*, 8*R*, 9*S*, 13*R*, 17*S*) absolute configuration was assigned from its 1D and 2D NOESY NMR spectra (Figure S15, Supporting Information). When evaluated against the HT-29 cell line,[30] **5g** did not show any activity (Table 5).

The mechanism of the formation of **5g** from **5** could be proposed based on the retro-Prins reaction.[35] As presumed in Scheme 1, isomerization of the *cis* a/b-ring system of **5** to a *trans* a/b-ring system was followed by hemiacetalization involving the C-3 hydroxy and C-10 formyl groups. Formate **5g** then could be formed via a retro-Prins reaction[35] of the intermediate hemiacetal. (Other related mechanisms for this reaction are also possible). Such a retro-Prins-type reaction based mechanism could also be extended to the biosynthesis of other 19-nor cardiac glycosides, as reported from *Antiaris toxicaria* recently.[36]

Investigation of the cytotoxicity of **1–5** and **5a–5g** showed that the C-3 saccharide residue, along with the C-5 and C-14 hydroxy and C-10 formyl groups, was important in the mediation of the cytotoxicity of **5** toward HT-29 cells, as indicated by the IC_{50} values (μM) of **5** (0.17) and **5g** (>20) (Table 5). Comparison of the data for **4** (IC_{50} 0.09 μM) with **2** (IC_{50} 0.69 μM) (Table 3) showed that different C-3 sugar residues contributed to the resultant activity differentially. Methylation of the 2′-hydroxy group decreased compound potency moderately, as shown by **3** (IC_{50} 0.36 μM) and **4** (IC_{50} 0.09 μM) (Table 3). The activity was reduced in a sequence following the bulk of the ester group when an acetyl, a benzoyl, or a 4-chlorobenzoyl group was introduced to 4'-OH of **5**, as implied by the IC_{50} values (μM) of **5** (0.17), **5a** (0.47), **5b** (1.2), and **5d** (2.8) (Table 5). Furthermore, the C-14 hydroxy group alone plays an important role in potentiating the cytotoxic effect against HT-29 cells, as indicated by comparison of **5d** (IC_{50} 2.8 μM) and **5f** (IC_{50} >20 μM) (Table 5). The activity was retained when the C-10 formyl group of **5** was reduced to a C-10 hydroxymethyl group, as indicated by the closely similar cytotoxicity of **1** (IC_{50} 0.16 μM) and **5** (IC_{50} 0.17 μM) (Table 3). However, oxidation of this formyl group to a hydroxycarbonyl group led to abolishment of the activity, as shown by data for **5b** (IC_{50} 1.2 μM) and **5c** (IC_{50} >20 μM), as well as **5d** (IC_{50} 2.8 μM) and **5e** (IC_{50} >20 μM) (Table 5).

Consistent with these observations, several cardiac glycosides were found previously to be more active than the corresponding aglycones,[36] and the activity against a small panel of human cancer cell lines was increased when the carbohydrate moiety was attached at both C-2 and C-3 through a 1,4-dioxane moiety.[20] No cytotoxicity was evident for several cardiac glycosides that contain a 17-hydroxy (IC_{50} > 40 μM)[19] or a 19-hydroxycarbonyl (IC_{50} > 10 μM) group.[28]

(+)-Strebloside (**5**), the main cytotoxic compound identified from the stem bark of *S. asper*, was tested further for its cytotoxicity toward the MDA-MB-435 human melanoma, MDA-MB-231 human breast cancer, and OVCAR3 human ovarian cancer cell lines.[37] It was found to be potently cytotoxic in all cases in the present study (Tables 3 and 6). Hence, (+)-strebloside (**5**) exhibits a broad spectrum of action toward both human solid tumor and leukemic cells.

(+)-Strebloside (**5**) was then deemed worthy of evaluation for its antitumor efficacy in an in vivo hollow fiber assay.[33] Immunodeficient NCr *nu/nu* mice were implanted with hollow fibers containing MDA-MB-231, MDA-MB-435, or OVCAR3 cells and treated with **5** at doses of 1.0, 5.0, 10.0, 15.0, or 30.0 mg/kg, or with the vehicle control or paclitaxel (positive control, 5 mg/kg). In all cases, intraperitoneal (ip) administration for four days was used. The relative cell survival values from the treatment of **5** at 5.0, 10.0, 15.0, or 30.0 mg/kg (ip) toward MDA-MB-231 cells and at 10.0, 15.0, or 30.0 mg/kg (ip) toward OVCAR3 cells were all statistically significantly different from those of the vehicle control (Figure 5). However, no efficacy was observed for **5** toward MDA-MB-435 cells using the same dose range (Figure S18, Supporting Information). The values from the treatment of **5** at all cases were significantly different from those of paclitaxel (Figure 5), and no gross toxicities were observed for any of the animals in this in vivo study. These results indicated that compound **5** showed activity toward MDA-MB-231 and OVCAR3 cells at doses down to 5 mg/kg and 10 mg/kg, respectively, although this efficacy was less potent than paclitaxel.

The cardiac glycoside drug digoxin is known to show a narrow therapeutic index[11] and has been administered (i.p.) to mice at a non-toxic dose of 0.7 mg/kg/day,[13] while its close analogue digitoxin exhibited an oral LD_{50} value of 10–80 mg/kg in mice.[38] (+)-Strebloside (**5**), however, did not exhibit obvious toxicity to the mice at doses (i.p.) up to 30 mg/kg, which is much higher than its effective dose of 5 mg/kg. Previously, several cardiac glycosides have been evaluated in clinical trials for the treatment of cancer,[7,15] and a mixture of two cardiac glycosides that contain the same cardenolide aglycone as **5** showed an LD_{50} value of more than 500 mg/kg in an acute oral toxicity test, using six-week old ddY mice.[38] Mechanistically, most cardiac glycosides mediate their cytotoxicity through inhibition of Na^+,K^+-ATPase followed by a Ca^{+2} flux pathway.[7,8,39] Therefore, (+)-strebloside (**5**) seems to be a promising lead compound worthy of further investigation for development as a new anticancer agent.

EXPERIMENTAL SECTION

General Experimental Procedures

Optical rotations were measured at room temperature on a Perkin-Elmer model 343 polarimeter with a path length of 10 mm. UV spectra were recorded on a Hitachi U2910 ultraviolet spectrophotometer. ECD measurements were performed using a JASCO J-810 spectropolarimeter. IR spectra were recorded on a Nicolet 6700 FT-IR spectrometer. ^1H and ^{13}C, DEPT 90, DEPT 135, HSQC, HMBC, NOESY, and COSY NMR spectra were recorded at room temperature on a Bruker Avance DRX 400, Bruker Avance II 400, Bruker Avance III HD 700, or a Bruker Avance III HD 800 MHz NMR spectrometer. ESIMS and HRESIMS data were collected on a Bruker Maxis 4G Q-TOF mass spectrometer in the positive-ion mode. Column chromatography was conducted using silica gel (65 × 250 or 230 × 400 mesh, Sorbent Technologies, Atlanta, GA, USA). Analytical thin-layer chromatography (TLC) was performed on precoated silica gel 60 F254 plates (Sorbent Technologies, Atlanta, GA, USA). Sephadex LH-20 was purchased from Amersham Biosciences, Uppsala, Sweden. For visualization of TLC plates, H_2SO_4 was used as spray reagent. All procedures were carried out using solvents purchased from commercial sources

and employed without further purification. Digoxin, paclitaxel, and other reagents for chemical synthesis were purchased from Sigma-Aldrich (St. Louis, MO, USA) (purity ≥ 98%).

Plant Material

A sample of the stem bark (acquisition number AA06920) of *S. asper* was collected in January 2010 by D.D.S. and T.N.N. (voucher specimen: *DDS 14729*) from a tree (eight-meters tall) at Dahang Village (11° 40.53' N; 109° 10.3' E), Nui Chua National Park, Ninh Hai District, Ninh Thuan Province, Vietnam. The voucher herbarium specimen has been deposited at the John G. Searle Herbarium of the Field Museum of Natural History, Chicago, IL, USA, under the accession numbers F-2294556.

Extraction and Isolation

The milled air-dried stem bark of *S. asper* (sample AA06920, 3100 g) was extracted with MeOH (4 L × 7) at room temperature. The solvent was evaporated in vacuo, and the dried MeOH extract (254.5 g, 8.2%) was resuspended in 10% H_2O in MeOH (1500 mL) and partitioned with *n*-hexane (1000, 600, and 500 mL) to yield an *n*-hexane-soluble residue (57.0 g, 1.8%). Then, 200 mL of H_2O were added to the aqueous MeOH layer, and this was partitioned with $CHCl_3$ (1000, 500, and 500 mL). The combined $CHCl_3$ partition was washed with a 1% aqueous solution of NaCl, to partially remove plant polyphenols, and the solvent was evaporated to afford a $CHCl_3$-soluble extract (13.0 g, 0.42%). The $CHCl_3$-soluble extract exhibited cytotoxicity toward the HT-29 cell line (IC_{50} < 1.0 μg/mL). Both the *n*-hexane- and water-soluble extracts were inactive (IC_{50} > 20.0 μg/mL) in the bioassay system used. The $CHCl_3$-soluble extract (12.5 g) was subjected to silica gel column chromatography (6.0 × 45 cm) and eluted with a gradient of *n*-hexane-acetone. Eluates were pooled by TLC analysis to give 19 combined fractions (D2F1–D2F19), and fractions D2F11–D2F19 were deemed active against HT-29 cells (IC_{50} < 1 μg/mL).

Fractions D2F11–D2F13 were combined and chromatographed over a silica gel column (4.5 × 40 cm), eluted with a gradient of CH_2Cl_2 (DCM)-MeOH to yield three pooled subfractions, D2F11F1–D2F11F3. Of these, fractions D2F11F2 and D2F11F3 were combined and further chromatographed over a silica gel column (4.5 × 40 cm), eluted with a gradient of DCM-MeOH, and purified by separation over a Sephadex LH-20 column, eluted with DCM-MeOH (1:1), affording (+)-strebloside (**5**, 420 mg).

Combined fractions D2F14–D2F16 were separated by silica gel chromatography (4.5 × 40 cm) eluted with a gradient of DCM-MeOH to yield two pooled subfractions, D2F14F1 and D2F14F2. Of these, fraction D2F14F1 was further chromatographed over a silica gel column (2.5 × 30 cm), eluted with a gradient of DCM-MeOH and purified by separation over a Sephadex LH-20 column, eluted with DCM-MeOH (1:1), to yield a further quantity of (+)-strebloside (**5**, 30 mg). Fraction D2F14F2 was separated over a series of silica gel columns (2.5 × 30 cm), eluted with a gradient mixture of DCM-MeOH, and purified by separation over Sephadex LH-20 columns, eluted with DCM -MeOH (1:1), to afford (+)-19-hydroxykamaloside (**1**, 20 mg), (+)-5-hydroxyasperoside (**2**, 2.0 mg), and (+)-3'-de-*O*-methylkamaloside (**3**, 1.0 mg).

Combined fractions D2F17–D2F19 were chromatographed over a silica gel column (2.5 × 30 cm), eluted with a gradient of DCM-MeOH, to yield two pooled subfractions, D2F17F1 and D2F17F2. Of these, fraction D2F17F1 was further chromatographed over a silica gel column (2.5 × 20 cm), eluted with a gradient of DCM-MeOH and purified by passage over a column containing Sephadex LH-20, eluted with DCM-MeOH (1:1), to yield an additional amount of (+)-19-hydroxykamaloside (**1**, 5.0 mg). Fraction D2F17F2 was separated over a series of silica gel columns (2.5 × 20 cm), eluted with a gradient of DCM-MeOH, and purified by separation over Sephadex LH-20 columns, eluted with DCM-MeOH (1:1), to afford (+)-3-*O*-*β*-D-fucopyranosylperiplogenin (**4**, 3.0 mg).

(+)-19-Hydroxykamaloside (1)—Amorphous colorless powder; $[\alpha]^{20}_{D}$ +13 (*c* 0.1, MeOH); UV (MeOH) λ_{max} (log ε) 216 (3.95) nm; ECD (MeOH, nm) λ_{max} (Δε) 238 (+2.76); IR (dried film) ν_{max} 3459, 2939, 1743, 1621, 1447, 1371, 1169, 1067 cm^{-1}; ^{1}H and ^{13}C NMR data, see Tables 1 and 2; positive-ion HRESIMS *m/z* 603.3153 (calcd for $C_{31}H_{48}O_{10}Na$, 603.3140).

(+)-5-Hydroxyasperoside (2)—Amorphous colorless powder; $[\alpha]^{20}_{D}$ +83 (*c* 0.1, MeOH); UV (MeOH) λ_{max} (log ε) 216 (4.13) nm; ECD (MeOH, nm) λ_{max} (Δε) 236 (+4.05); IR (dried film) ν_{max} 3445, 2928, 1739, 1627, 1450, 1378, 1274, 1077 cm^{-1}; ^{1}H and ^{13}C NMR data, see Tables 1 and 2; positive-ion HRESIMS *m/z* 603.3152 (calcd for $C_{31}H_{48}O_{10}Na$, 603.3140).

(+)-3'-De-O-methylkamaloside (3)—Amorphous colorless powder; $[\alpha]^{20}_{D}$ +50 (*c* 0.1, MeOH); UV (MeOH) λ_{max} (log ε) 216 (4.08) nm; ECD (MeOH, nm) λ_{max} (Δε) 241 (+3.99); IR (dried film) ν_{max} 3479, 2931, 1743, 1621, 1449, 1365, 1222, 1166, 1079 cm^{-1}; ^{1}H and ^{13}C NMR data, see Tables 1 and 2; positive-ion HRESIMS *m/z* 573.3054 (calcd for $C_{30}H_{46}O_{9}Na$, 573.3034).

Acetylation of (+)-Strebloside (5)

To a dried 25 mL glass vial equipped with a magnetic stirrer, containing 11.6 mg (0.02 mmol) of (+)-strebloside (**5**), 50 μL of Ac_2O and 1 mL pyridine were added, and the vial was sealed. After the mixture was stirred at 70 °C for 1 h, it was cooled to room temperature. Then, DCM (5 mL) was added, and the solution was extracted with distilled H_2O. The organic layer was washed with distilled H_2O, and evaporated at reduced pressure. The residue was purified by silica gel column chromatography, using *n*-hexane-acetone (5:1→1:1), to afford 8.0 mg (0.013 mmol) of **5a** (64.5%).

(+)-4'-O-Acetylstrebloside or (3β,5β)-3-[(2,3-Di-O-methyl-4-O-acetyl-β-D-fucopyranosyl)oxy]-5,14-dihydroxy-19-oxocard-20(22)-enolide (5a)—Amorphous colorless powder; $[\alpha]^{20}_{D}$ +20 (*c* 0.1, MeOH); UV (MeOH) λ_{max} (log ε) 216 (3.96) nm; ECD (MeOH, nm) λ_{max} (Δε) 235 (+2.46); IR (dried film) ν_{max} 3501, 2940, 1747, 1622, 1447, 1374, 1239, 1067 cm^{-1}; ^{1}H and ^{13}C NMR data, see Table S1 (Supporting Information); positive-ion HRESIMS *m/z* 643.3109 (calcd for $C_{33}H_{48}O_{11}Na$, 643.3094).

Benzoylation of (+)-Strebloside (5)

To a dried 25 mL glass vial equipped with a magnetic stirrer, containing 17.3 mg (0.03 mmol) of (+)-strebloside (**5**), 1 mL (8.6 mmol) of benzoyl chloride and 100 μL of pyridine were added, and the vial was sealed. After the mixture was stirred at 70 °C for 1 h, it was cooled to room temperature. Then, DCM (5 mL) was added, and the solution was extracted with distilled H_2O. The organic layer was washed with distilled H_2O, and evaporated at reduced pressure. The residue was purified by silica gel column chromatography, using *n*-hexane-acetone (5:1→1:1), to afford 2.0 mg (0.003 mmol) of **5b** (10%) and 3.0 mg (0.004 mmol) of **5c** (14.3%).

(+)-4'-O-Benzoylstrebloside or (3β,5β)-3-[(2,3-Di-O-methyl-4-O-benzoyl-β-D-fucopyranosyl)oxy]-5,14-dihydroxy-19-oxocard-20(22)-enolide (5b)—Amorphous colorless powder; $[\alpha]^{20}_D$ +10 (*c* 0.1, MeOH); UV (MeOH) λ_{max} (log ε) 222 (3.97) nm; ECD (MeOH, nm) λ_{max} (Δε) 235 (+2.02); IR (dried film) ν_{max} 3501, 2926, 1722, 1621, 1452, 1383, 1275, 1161, 1068 cm^{-1}; ^1H and ^{13}C NMR data, see Tables S2 and S3 (Supporting Information); positive-ion HRESIMS *m/z* 705.3260 (calcd for $C_{38}H_{50}O_{11}Na$, 705.3245).

(+)-4'-O-Benzoyl-19-nor-kamaloside-10-carboxylic acid or (3β,5β,14β)-3-[(2,3-Di-O-methyl-4-O-benzoyl-β-D-fucopyranosyl)oxy]-5,14,21-trihydroxy-24-norchol-20(22)-ene-19,23-dioic acid-γ-lactone (5c)—Amorphous colorless powder; $[\alpha]^{20}_D$ +30 (*c* 0.1, MeOH); UV (MeOH) λ_{max} (log ε) 224 (4.02) nm; ECD (MeOH, nm) λ_{max} (Δε) 235 (+4.83); IR (dried film) ν_{max} 3501, 2936, 1723, 1621, 1451, 1383, 1275, 1161. 1068 cm^{-1}; ^1H and ^{13}C NMR data, see Tables S2 and S3 (Supporting Information); positive-ion HRESIMS *m/z* 721.3214 (calcd for $C_{38}H_{50}O_{12}Na$, 721.3194).

4-Chlorobenzoylation of (+)-Strebloside (5)

To a dried 25 mL glass vial equipped with a magnetic stirrer, containing 17.3 mg (0.03 mmol) of (+)-strebloside (**5**), 216 μL (1.5 mmol) of 4-chlorobenzoyl chloride, 100 μL of pyridine, and 5 mL of DCM were added, and the vial was sealed. After the mixture was stirred at room temperature overnight, DCM (5 mL) was added, and the solution was extracted with distilled H_2O. The organic layer was washed with distilled H_2O, and evaporated at reduced pressure. The residue was purified by silica gel column chromatography, using *n*-hexane-acetone (5:1→1:1), to afford 2.5 mg (0.0035 mmol) of **5d** (11.9%), 5.0 mg (0.007 mmol) **5e** (22.7%), and 3.0 mg (0.004 mmol) of **5f** (13.9%).

(+)-4'-O-(4-Chlorobenzoyl)strebloside or (3β,5β)-3-{[2,3–Di-O-methyl-4-O-(4-chloro)benzoyl-β-D-fucopyranosyl]oxy}-5,14-dihydroxy-19-oxocard-20(22)-enolide (5d)—Amorphous colorless powder; $[\alpha]^{20}_D$ +20 (*c* 0.1, MeOH); UV (MeOH) λ_{max} (log ε) 238 (3.87), 201 (4.11) nm; ECD (MeOH, nm) λ_{max} (Δε) 237 (+2.31); IR (dried film) ν_{max} 3501, 2922, 1744, 1729, 1622, 1591, 1455, 1380, 1273, 1169, 1092 cm^{-1}; ^1H and ^{13}C NMR data, see Tables S2 and S3 (Supporting Information); positive-ion HRESIMS *m/z* 739.2862 (calcd for $C_{38}H_{49}O_{11}ClNa$, 739.2856).

(+)-4'-O-(4-Chlorobenzoyl)-19-nor-kamaloside-10-carboxylic acid or (3β,5β,14β)-3-{[2,3–Di-O-methyl-4-O-(4-chloro)benzoyl-β-D-fucopyranosyl]oxy}-5,14,21-trihydroxy-24-norchol-20(22)-ene-19,23-dioic acid-γ-lactone (5e)—Amorphous colorless powder; $[\alpha]^{20}_{D}$ +20 (*c* 0.1, MeOH); UV (MeOH) λ_{max} (log ε) 233 (4.10), 201 (4.33) nm; ECD (MeOH, nm) λ_{max} (Δε) 237 (+2.31); IR (dried film) ν_{max} 3508, 2926, 1731, 1622, 1594, 1447, 1338, 1273, 1067 cm^{-1}; ^{1}H and ^{13}C NMR data, see Tables S2 and S3 (Supporting Information); positive-ion HRESIMS *m/z* 755.2805 (calcd for $C_{38}H_{49}O_{12}ClNa$, 755.2805).

(+)-4'-O-(4-Chlorobenzoyl)-14(15)-anhydrostrebloside or (3β,5β)-3-{[2,3–Di-O-methyl-4-O-(4-chloro)benzoyl-β-D-fucopyranosyl]oxy}-5-hydroxy-19-oxocard-14(15),20(22)-dienolide (5f)—Amorphous colorless powder; $[\alpha]^{20}_{D}$ +10 (*c* 0.1, MeOH); UV (MeOH) λ_{max} (log ε) 238 (3.86), 201 (4.17) nm; ECD (MeOH, nm) λ_{max} (Δε) 239 (–2.34), 216 (+3.28); IR (dried film) ν_{max} 3508, 2931, 1749, 1716, 1629, 1594, 1488, 1337, 1273, 1170, 1092 cm^{-1}; ^{1}H and ^{13}C NMR data, see Table S4 (Supporting Information); positive-ion HRESIMS *m/z* 721.2753 (calcd for $C_{38}H_{47}O_{10}ClNa$, 721.2750).

Acid Hydrolysis of (+)-Strebloside (5)

To a 25 mL glass vial equipped with a magnetic stirrer, containing 17.3 mg (0.03 mmol) of (+)-strebloside (**5**), 775 μL (10 mmol) of trifluoroacetic acid and 5 mL of acetone were added, and the vial was sealed. After the mixture was stirred at 70 °C for 1 h, it was cooled to room temperature. Then, DCM (5 mL) was added, and the solution was extracted with distilled H_2O. The organic layer was washed with distilled H_2O, and evaporated at reduced pressure. The residue was purified by silica gel column chromatography, using *n*-hexane-acetone (5:1→1:1), to afford 2.0 mg (0.005 mmol) of **5g** (18.0%).

(+)-19-Nor-5(10),14-dianhydrostrophanthidin-3-yl formate or (3β)-3-O-Formyl-19-nor-card-5(10),14(15),20(22)-trienolide (5g)—Amorphous colorless powder; $[\alpha]^{20}_{D}$ +10 (*c* 0.1, MeOH); UV (MeOH) λ_{max} (log ε) 209 (3.64) nm; ECD (MeOH, nm) λ_{max} (Δε) 242 (–2.51), 213 (+4.67); IR (dried film) ν_{max} 3445, 2924, 1747, 1629, 1453, 1378, 1181, 1044 cm^{-1}; ^{1}H and ^{13}C NMR data, see Table S4 (Supporting Information); positive-ion HRESIMS *m/z* 391.1899 (calcd for $C_{23}H_{28}O_4Na$, 391.1880).

Determination of Absolute Configuration of the 1,2-Diol Unit of Digoxin

The ECD spectra of digoxin (1.0 mM in a DMSO solution) and $[Mo_2(OAc)_4]$ (1.2 mM in a DMSO solution), and the induced ECD spectrum of digoxin [1.0 mM in a $[Mo_2(OAc)_4]$ (1.2 mM) DMSO solution for 20 min) were measured on a JASCO J-810 spectropolarimeter in a 0.5 cm cell from 500 nm to 270 nm under identical conditions. The relation between the absolute configuration of the 1,2-diol moiety of digoxin and the sign of the O-C-C-O dihedral angles was performed following a reported procedure.[24] $[Mo_2(OAc)_4]$ (Sigma-Aldrich) and DMSO (Sigma Aldrich, anhydrous ≥99.9%) were commercially available and used without further purification.

Cell Lines and Peripheral Blood Cells

All cell lines were purchased from the American Type Culture Collection (ATCC, Manassas, VA, USA). Peripheral blood was obtained from healthy human donors under an Institutional Review Board-approved protocol from the Ohio State University (2016C0032), and mononuclear cells were isolated by Ficoll density gradient centrifugation. The HT-29 human colon cancer cell line was cultured in MEME medium (Hyclone, Logan, UT, USA) supplemented with heat-inactivated fetal bovine serum (FBS, 10%), penicillin (100 units/mL), streptomycin (100 μg/mL), and amphotericin B (fungizone, 0.25 μg/mL). The human MV4–11 and Kasumi-1 myeloid leukemia cell lines and normal human peripheral blood mononuclear cells were cultured in RPMI 1640 medium (Invitrogen, Carlsbad, CA, USA), supplemented with FBS (20%), penicillin (100 units/mL), and streptomycin (100 μg/mL). The MDA-MB-231 human breast cancer, MDA-MB-435 human melanoma, and OVCAR3 human ovarian cancer cell lines were cultured in RPMI 1640 medium, supplemented with FBS (10%), penicillin (100 units/mL), and streptomycin (100 μg/mL). The H1299 human non-small cell lung cancer cell line was maintained in Dulbecco's Modified Eagle Medium (DMEM containing 25 mM glucose) supplemented with FBS (10%), penicillin (100 units/mL), and streptomycin (100 μg/mL). The CCD-112CoN normal human colon cell line was cultured in MEME medium supplemented with FBS (10%), penicillin G-streptomycin-fungizone solution (PSF, 1%), 1.0 mM sodium pyruvate, 0.1 mM non-essential amino acid, and 1.5 g/L sodium bicarbonate. The NL20 normal human lung cell line was maintained in Ham's F12 medium, supplemented with FBS (4%), penicillin (100 units/mL), and streptomycin (100 μg/mL), 0.1 mM non-essential amino acids, 0.005 mg/mL insulin, 10 ng/mL epidermal growth factor, 0.001 mg/mL transferrin, and 500 ng/mL hydrocortisone. All cultures were maintained at 37 °C in 5% CO_2.

Cytotoxicity Assay against the HT-29 Cell Line

The cytotoxicity of the test compounds and digoxin was screened against HT-29 cells by a previously reported procedure,[30] with the vehicle and paclitaxel used as the negative and positive control, respectively.

Cytotoxicity Assay toward Human Leukemia Cells and Effect of Testing against Normal Human Peripheral Blood Mononuclear Cells

Cell growth inhibition/cytotoxicity was evaluated after 48 h incubation by an MTS assay (CellTiter 96, Promega, Madison WI, USA), using silvestrol.[31] Briefly, MV4–11, Kasumi-1, or normal human peripheral blood mononuclear cells were seeded in 96-well plates and incubated with test samples or silvestrol (both dissolved in DMSO and diluted to different concentrations) or the vehicle (DMSO) for 48 h. Then, 20 μL of the CellTiter 96 reagent were added to each well. After an additional 4 h incubation, the optical density at 490 nm was measured, with IC_{50} values calculated with respect to the control samples.

Cytotoxicity Assay against the H1299 and NL20 Cell Lines

This assay was performed against the H1299 human non-small cell lung cancer and human non-tumorigenic NL20 lung cell lines using a reported procedure.[32] Cell growth or proliferation was assessed using the MTT proliferation assay kit (Cayman, Ann Arbor, MI,

USA). Briefly, 5000 cells were seeded in each well of a 96-well plate and cells were treated with or without test compounds. After cells were cultured for 24 h, they were treated with MTT for 4 h. Then, the medium was removed, and 100 μL Crystal Dissolving Solution was added to each well. The absorbance of the solution was measured at 570 nm, with IC_{50} values calculated from the vehicle control.

Cytotoxicity Assay against the CCD-112CoN Cell Line

Following a procedure reported previously,[33] the cytotoxicity of compound **5**, along with commercial digoxin, was screened against the CCD-112CoN cell line.

Cytotoxicity Assay against MDA-MB-231, MDA-MB-435, or OVCAR3 Cell Lines

Following a protocol used previously,[37] MDA-MB-231, MDA-MB-435, or OVCAR3 cells in log phase growth were harvested by trypsinization and seeded in 96-well clear flat-bottomed plates (Microtest 96, Falcon). Cells were incubated at 37 °C in 5% CO_2 overnight and then treated with the samples or paclitaxel (the positive control) (both dissolved in DMSO and diluted to different concentrations required) or the vehicle (DMSO) for 72 h. Viability of cells was evaluated by a commercial absorbance assay (CellTiter 96 AQueous One Solution Cell Proliferation Assay, Promega Corp, Madison, WI, USA), with the IC_{50} values calculated from the vehicle control.

Animals

Seven-week-old immunodeficient NCr *nu/nu* mice were purchased from The Jackson Laboratory (Bar Harbor, ME, USA) and housed in cages at room temperature with a relative humidity of 50–60% under 12:12 h light–dark cycle. This procedure was approved by the University of Illinois at Chicago Animal Care and Use Committee (protocol number 13-057), and the mice were treated in accordance with the institutional guidelines for animal care.

In Vivo Hollow Fiber Assay

An in vivo hollow fiber assay was performed for the evaluation of antitumor efficacy of **5** using procedures previously described in detail.[33] In brief, seven-week-old immunodeficient NCr *nu/nu* mice were divided into seven groups, including a vehicle negative control group (12 mice), a paclitaxel positive control group (12 mice), and (+)-strebloside (**5**) treatment groups with dose of 1, 5, 10, 15, and 30 mg/kg, respectively (six mice for each group treated with compound **5**). (+)-Strebloside (**5**) was dissolved initially in EtOH and subsequently diluted with Tween 20. The mixture was diluted with distilled water to 5% EtOH and 5% Tween 20. Hollow fibers containing MDA-MB-231, MDA-MB-435, or OVCAR3 cells were implanted into the abdominal cavity of mice on day 0. The mice were injected i.p. once daily for four days (from day 3 to day 6) with **5** (different dose as indicated) and the vehicle negative and paclitaxel (5 mg/kg) positive controls, respectively. On day 7, all the remaining mice were sacrificed. The fibers were retrieved, and viable cell mass was evaluated by a modified MTT [3-(4,5-dimethylthiazol-2-yl)-2,5-diphenyltetrazolium bromide] assay. The percentage of the net growth for the cells in each treatment group was calculated by subtracting the day 0 absorbance from the day 7 absorbance and dividing this difference by

the net growth in the vehicle control (minus value between the day 7 and the day 0) (Figure 5). Each mouse was weighed daily during the study, and no signs of toxicity was found among the test animals even at the highest treatment dose (30 mg/kg) of **5**.

Statistical Analysis

The in vitro measurements were performed in triplicate and are representative of three independent experiments, where the values generally agreed within 10%. The dose response curve was calculated for IC_{50} determinations using non-linear regression analysis (Table Curve2DV4; AISN Software Inc. Mapleton, OR, USA). Differences among samples were assessed by one-way ANOVA followed by Tukey-Kramer's test, and the significance level was set at $p < 0.05$. The data from an in vivo hollow fiber assay were analyzed with linear mixed effect models to take account of the correlation of the observations from the same trial. Holm's procedure was used to adjust for multiple comparisons of the multiple doses used for the same cell line. An adjusted p value less than 0.05 was considered statistically significant.

Supplementary Material

Refer to Web version on PubMed Central for supplementary material.

Acknowledgments

This investigation was supported by grant P01 CA125066 and by grant P30 CA016058 funded by the National Cancer Institute, NIH, Bethesda, MD. The plant sample of *Streblus asper* was collected under a collaborative arrangement between the University of Illinois at Chicago (USA) and the Institute of Ecology and Biological Resources of the Vietnam Academy of Science and Technology, Hanoi (Vietnam). We thank Drs. David J. Hart and Judith C. Gallucci, Department of Chemistry and Biochemistry, The Ohio State University, for the helpful comments and suggestions about the mechanism of the formation of compound **5g** and the crystal structure of digoxin, respectively. We thank Dr. Chia-Hsien Wu, Division of Medicinal Chemistry and Pharmacognosy, College of Pharmacy, The Ohio State University, for his help for the chemical synthesis. Drs. Arpad Somogy, Nanette M. Kleinholz, and Yu Cao of the Mass Spectrometry and Proteomics of the Campus Chemical Instrument Center, The Ohio State University, are thanked for acquisition of the MS data. Drs. Craig A. McElroy (College of Pharmacy) and Chunhua Yuan (Nuclear Magnetic Resonance Laboratory, Campus Chemical Instrument Center), The Ohio State University, are thanked for access to some of the NMR instrumentations used in this investigation and for the 700 or 800 MHz NMR measurements, respectively.

REFERENCES

1. Datwyler SL, Weiblen GD. Am. J. Bot. 2004; 91:767–777. [PubMed: 21653431]
2. Suresh Kumar RB, Kar B, Dolai N, Karmakar I, Bhattacharya S, Haldar PK. Interdiscip. Toxicol. 2015; 8:125–130. [PubMed: 27486371]
3. Khare MP, Bhatnagar SS, Schindler O, Reichstein T. Helv. Chim. Acta. 1962; 45:1515–1534.
4. Saxena VK, Chaturvedi SK. Planta Med. 1985:343–344. [PubMed: 17340531]
5. Fiebig M, Duh C-Y, Pezzuto JM, Kinghorn AD, Farnsworth NR. J. Nat. Prod. 1985; 48:981–985. [PubMed: 4093781]
6. Hano Y, Juma P, Abliz Z, Sun H-D, Nomura T. Heterocycles. 2003; 59:805–809.
7. Newman RA, Yang P, Pawlus AD, Block KI. Mol. Intervent. 2008; 8:36–49.
8. Slingerland M, Cerella C, Guchelaar HJ, Diederich M, Gelderblom H. Invest. New Drugs. 2013; 31:1087–1094. [PubMed: 23748872]
9. Smith S. J. Chem. Soc. 1930:508–510.
10. Go K, Kartha G. Acta Cryst. 1980; B36:1811–1819.
11. Eichhorn EJ, Gheorghiade M. Prog. Cardiovasc. Dis. 2002; 44:251–266. [PubMed: 12007081]

12. Stenkvist B, Bengtsson E, Eriksson O, Holmquist J, Nordin B, Westman-Naeser S. Lancet. 1979; 313:563.
13. Svensson A, Azarbayjani F, Bäckman U, Matsumoto T, Christofferson R. Anticancer Res. 2005; 25:207–212. [PubMed: 15816540]
14. Platz EA, Yegnasubramanian S, Liu JO, Chong CR, Shim JS, Kenfield SA, Stampfer MJ, Willett WC, Giovannucci E, Nelson WG. Cancer Discov. 2011; 1:68–77. [PubMed: 22140654]
15. Cragg GM, Grothaus PG, Newman DJ. J. Nat. Prod. 2014; 77:703–723. [PubMed: 24499205]
16. Felth J, Rickardson L, Rosén J, Wickström M, Fryknäs M, Lindskog M, Bohlin L, Gullbo J. J. Nat. Prod. 2009; 72:1969–1974. [PubMed: 19894733]
17. Kinghorn AD, Carcache de Blanco EJ, Chai H-B, Orjala J, Farnsworth NR, Soejarto DD, Oberlies NH, Wani MC, Kroll DJ, Pearce CJ, Swanson SM, Kramer RA, Rose WC, Fairchild CR, Vite GD, Emanuel S, Jarjoura D, Cope FO. Pure Appl. Chem. 2009; 81:1051–1063. [PubMed: 20046887]
18. Wang T-M, Hojo T, Ran F-X, Wang R-F, Wang R-Q, Chen H-B, Cui J-R, Shang M-Y, Cai S-Q. J. Nat. Prod. 2007; 70:1429–1433. [PubMed: 17844995]
19. Araya JJ, Kindscher K, Timmermann BN. J. Nat. Prod. 2012; 75:400–407. [PubMed: 22316168]
20. Zhang R-R, Tian H-Y, Tan Y-F, Chung T-Y, Sun X-H, Xia X, Ye W-C, Middleton DA, Fedosova N, Esmann M, Tzen JTC, Jiang R-W. Org. Biomol. Chem. 2014; 12:8919–8929. [PubMed: 25270760]
21. Gottlieb HE, Kotlyar V, Nudelman A. J. Org. Chem. 1997; 62:7512–7515. [PubMed: 11671879]
22. Aulabaugh AE, Crouch RC, Martin GE, Ragouzeos A, Shockcor JP, Spitzer TD, Farrant RD, Hudson BD, Lindon JC. Carbohydr. Res. 1992; 230:201–212. [PubMed: 1394296]
23. Macrae CF, Bruno IJ, Chisholm JA, Edgington PR, McCabe P, Pidcock E, Rodriguez-Monge L, Taylor R, van de Streek J, Wood PA. J. Appl. Cryst. 2008; 41:466–470.
24. Frelek J, Ikekawa N, Takatsuto S, Snatzke G. Chirality. 1997; 9:578–582.
25. Gil RR, Lin L-Z, Chai H-B, Pezzuto JM, Cordell GA. J. Nat. Prod. 1995; 58:848–856. [PubMed: 7673928]
26. Seidl PR, Tostes JGR, Carneiro JWdeM, Taft CA, Dias JF. J. Mol. Struct. (Theochem). 2001; 539:163–169.
27. Junior P, Wichtl M. Phytochemistry. 1980; 19:2193–2197.
28. Tian D-M, Cheng H-Y, Jiang M-M, Shen W-Z, Tang J-S, Yao X-S. J. Nat. Prod. 2016; 79:38–50. [PubMed: 26714048]
29. Rovinski JM, Tewalt GL, Sneden AT. J. Nat. Prod. 1987; 50:211–216. [PubMed: 3655796]
30. Ren Y, Matthew S, Lantvit DD, Ninh TN, Chai H-B, Fuchs JR, Soejarto DD, Carcache de Blanco EJ, Swanson SM, Kinghorn AD. J. Nat. Prod. 2011; 74:1117–1125. [PubMed: 21428375]
31. Alachkar H, Santhanam R, Harb JG, Lucas DM, Oaks JJ, Hickey CJ, Pan L, Kinghorn AD, Caligiuri MA, Perrotti D, Byrd JC, Garzon R, Grever MR, Marcucci G. J. Hematol. Oncol. 2013; 6:21. [PubMed: 23497456]
32. Liu Y, Cao Y, Zhang W, Bergmeier S, Qian Y, Akbar H, Colvin R, Ding J, Tong L, Wu S, Hines J, Chen X. Mol. Cancer Ther. 2012; 11:1672–1682. [PubMed: 22689530]
33. Ren Y, Lantvit DD, Deng Y, Kanagasabai R, Gallucci JC, Ninh TN, Chai H-B, Soejarto DD, Fuchs JR, Yalowich JC, Yu J, Swanson SM, Kinghorn AD. J. Nat. Prod. 2014; 77:1494–1504. [PubMed: 24937209]
34. Emanuelsson R, Löfås H, Wallner A, Nauroozi D, Baumgartner J, Marschner C, Ahuja R, Ott S, Grigoriev A, Ottosson H. Chem Eur. J. 2014; 20:9304–9311. [PubMed: 25043852]
35. Al-Qallaf FAH, Johnstone RAW, Liu J-Y, Lu L, Whittaker D. J. Chem. Soc. Perkin Trans. 1999; 2:1421–1423.
36. Shi L-S, Kuo S-C, Sun H-D, Morris-Natschke SL, Lee K-H, Wu T-S. Bioorg. Med. Chem. 2014; 22:1889–1898. [PubMed: 24582402]
37. Zhao M, Onakpa MM, Santarsiero BD, Chen W-L, Szymulanska-Ramamurthy KM, Swanson SM, Burdette JE, Che C-T. J. Nat. Prod. 2015; 78:2731–2737. [PubMed: 26523419]
38. Goda Y, Sakai S, Nakamura T, Akiyama H, Toyoda M. Shokuhin Eiseigaku Zasshi. 1998; 39:256–265.

39. Durlacher CT, Chow K, Chen X-W, He Z-X, Zhang X, Yang T, Zhou S-F. Clin. Exp. Pharmacol. Physiol. 2015; 42:427–443. [PubMed: 25739707]

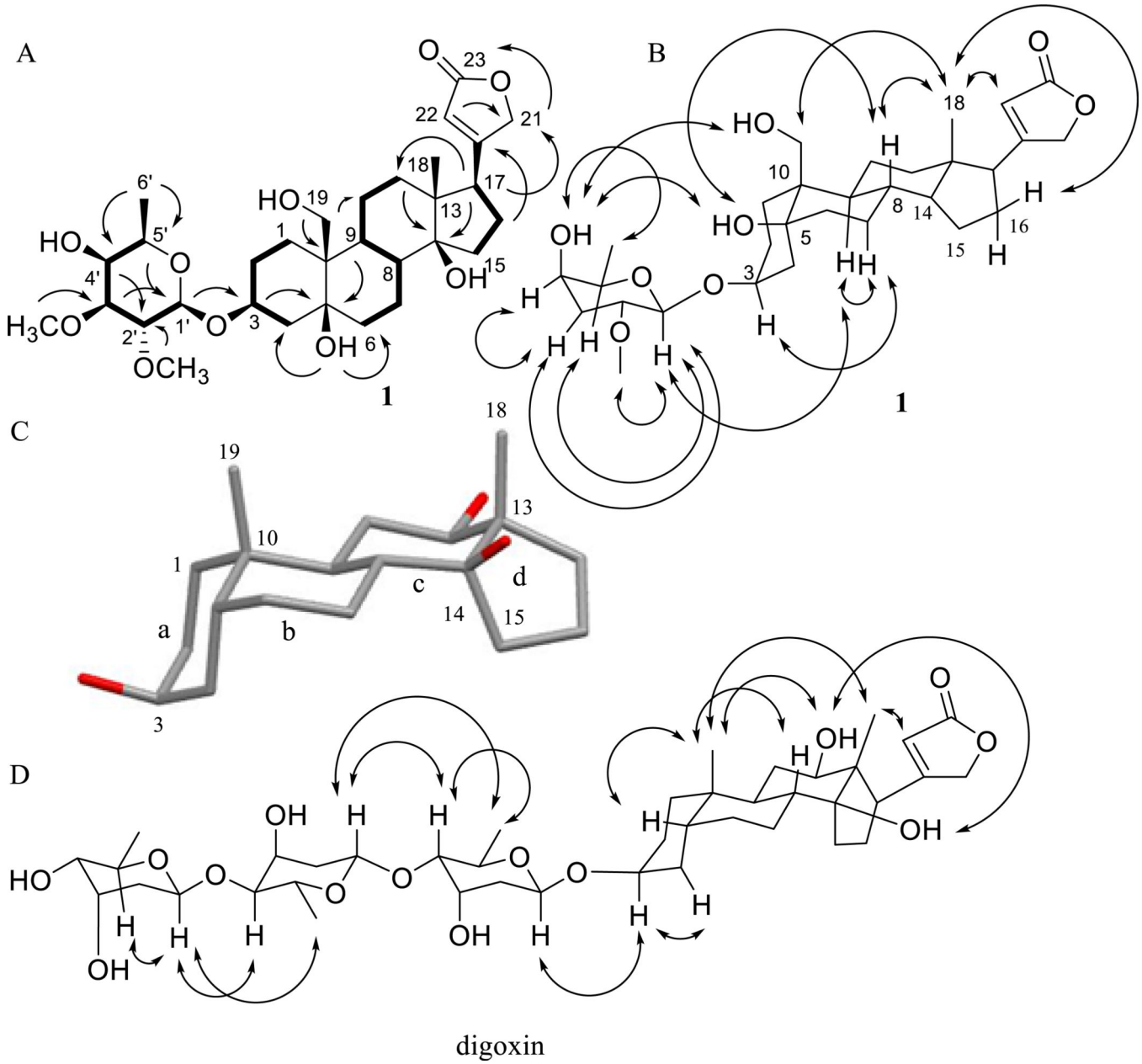

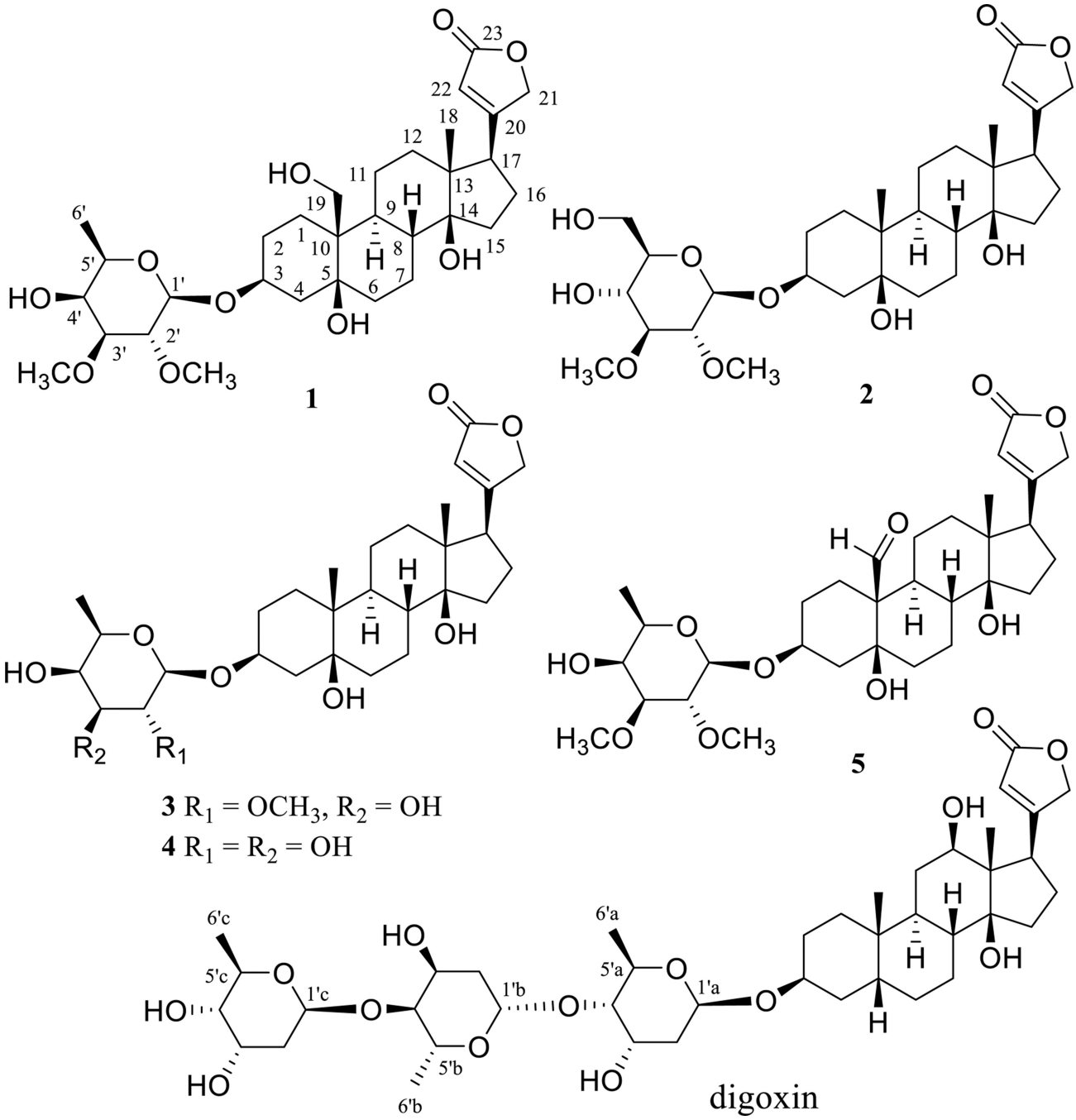

Figure 1.

A. COSY (▬, $^1H \rightarrow {}^1H$) and key HMBC (↷, $^1H \rightarrow {}^{13}C$) correlations of **1**. B. Selected NOESY (↷, $^1H \rightarrow {}^1H$) correlations of **1**. C. Partial structure showing the conformation of the central ring system as generated by *Mercury* CSD Version 3.1.1,[23] and based on the reported crystal structure of digoxin.[10] D. Selected NOESY (↷, $^1H \rightarrow {}^1H$) correlations of digoxin.

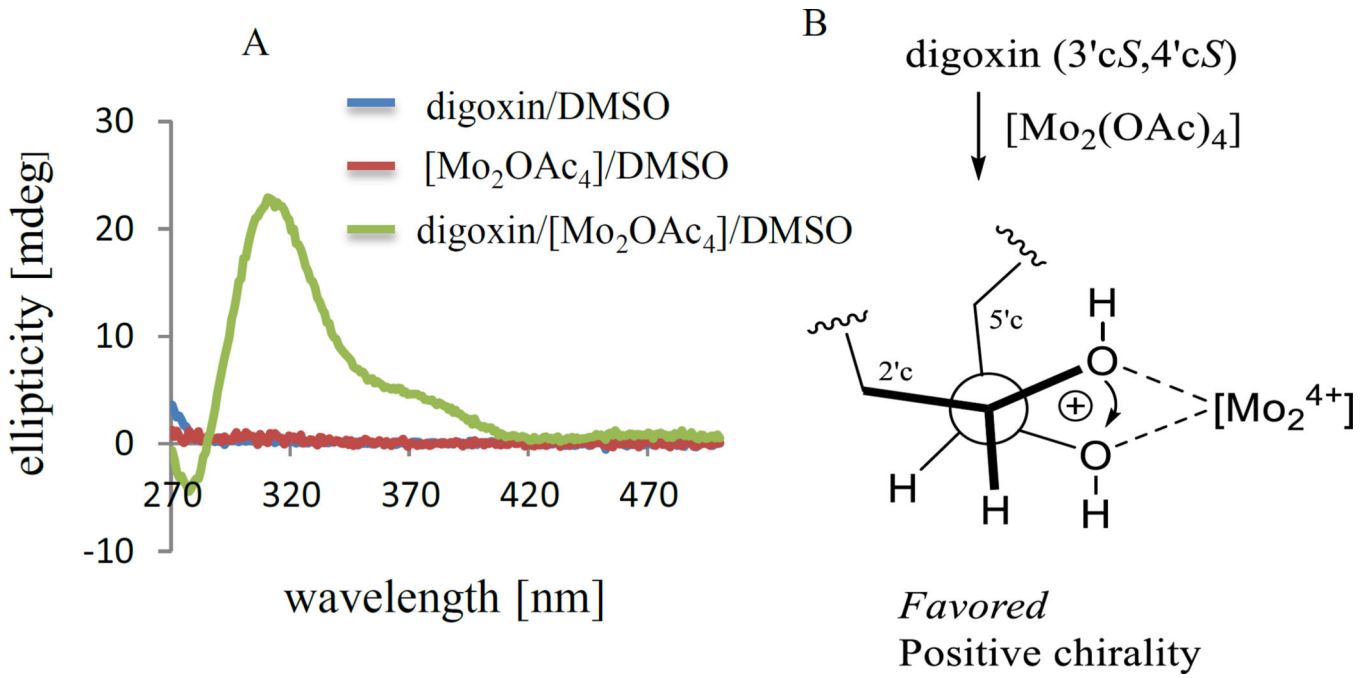

Figure 2.

A. ECD spectrum of digoxin induced by $[Mo_2(OAc)_4]$ (IECD, 1.0 mM digoxin in a 1.2 mM DMSO solution of dimolybdenum tetraacetate $[(MoAc_2)_2]$, 1.2 mM, in DMSO). B. The relationship between the absolute configuration of C-3'c and 4'c of digoxin and the sign of the O-C-C-O dihedral angle.

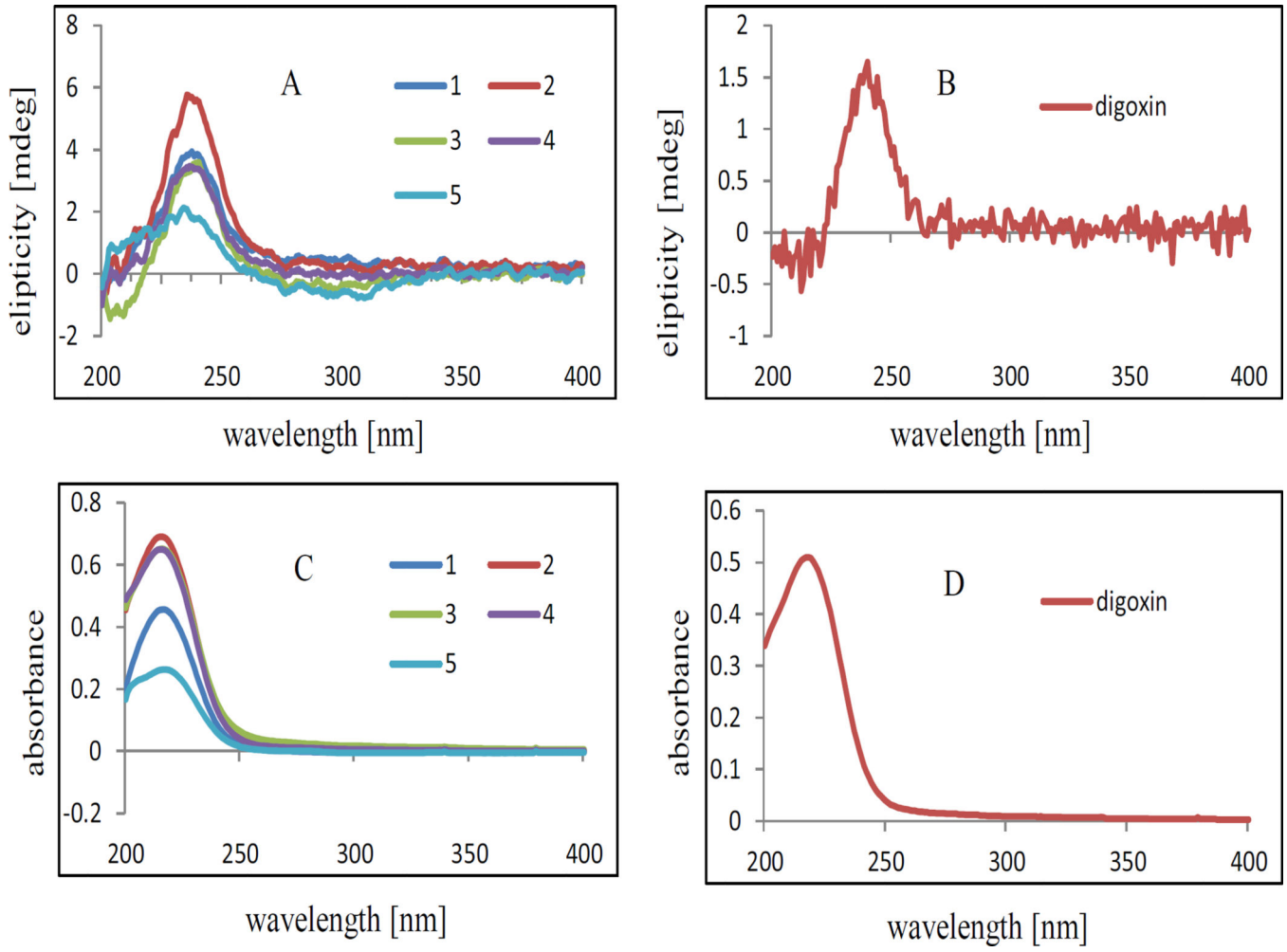

Figure 3.
ECD (A and B) and UV (C and D) spectra of compounds **1–5** and digoxin.

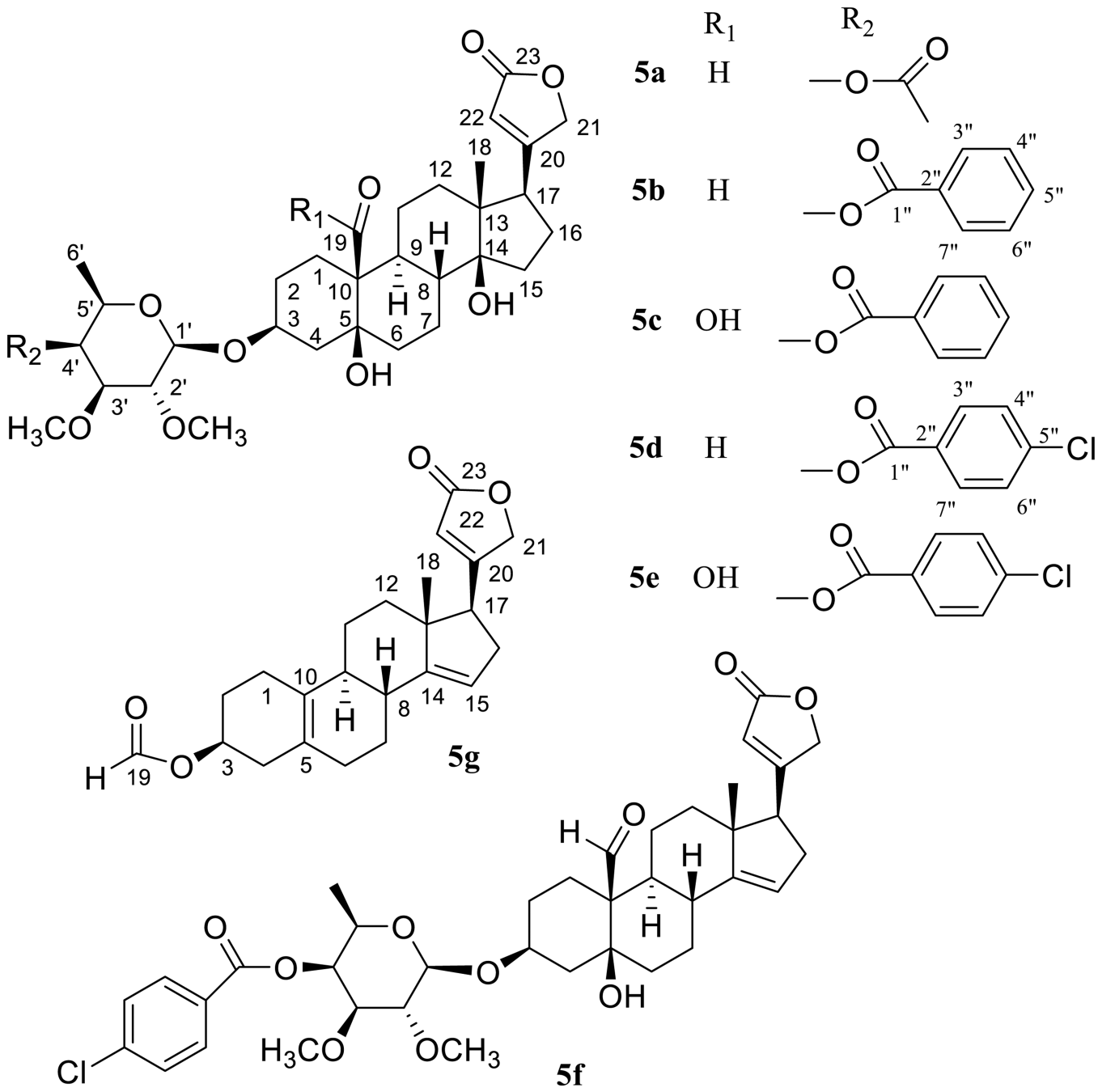

Figure 4.
Structure of synthesized derivatives of (+)-strebloside (**5**).

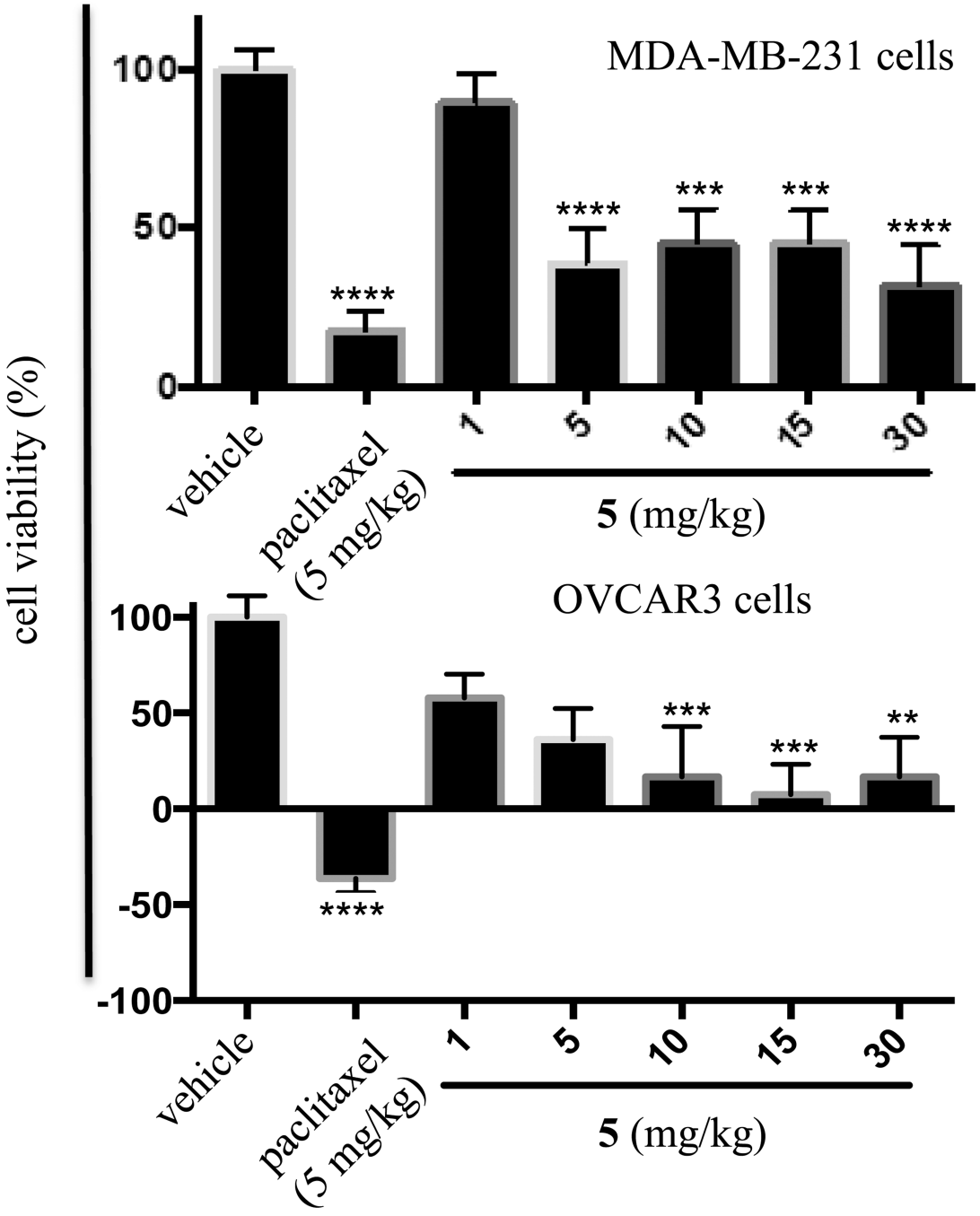

Figure 5.

Effect of (+)-strebloside (**5**) on the growth of human breast MDA-MB-231 and ovarian OVCAR3 cancer cells implanted in NCr *nu/nu* mice tested in an in vivo hollow fiber assay. The results are shown as the average percentage cell growth relative to control [columns, mean in each group ($n = 12$ for the control group and $n = 6$ for the treatment group); bars, SE; **$p \leq 0.05$, ***$p \leq 0.01$, and ****$p \leq 0.001$ for significant differences from the control treatment.

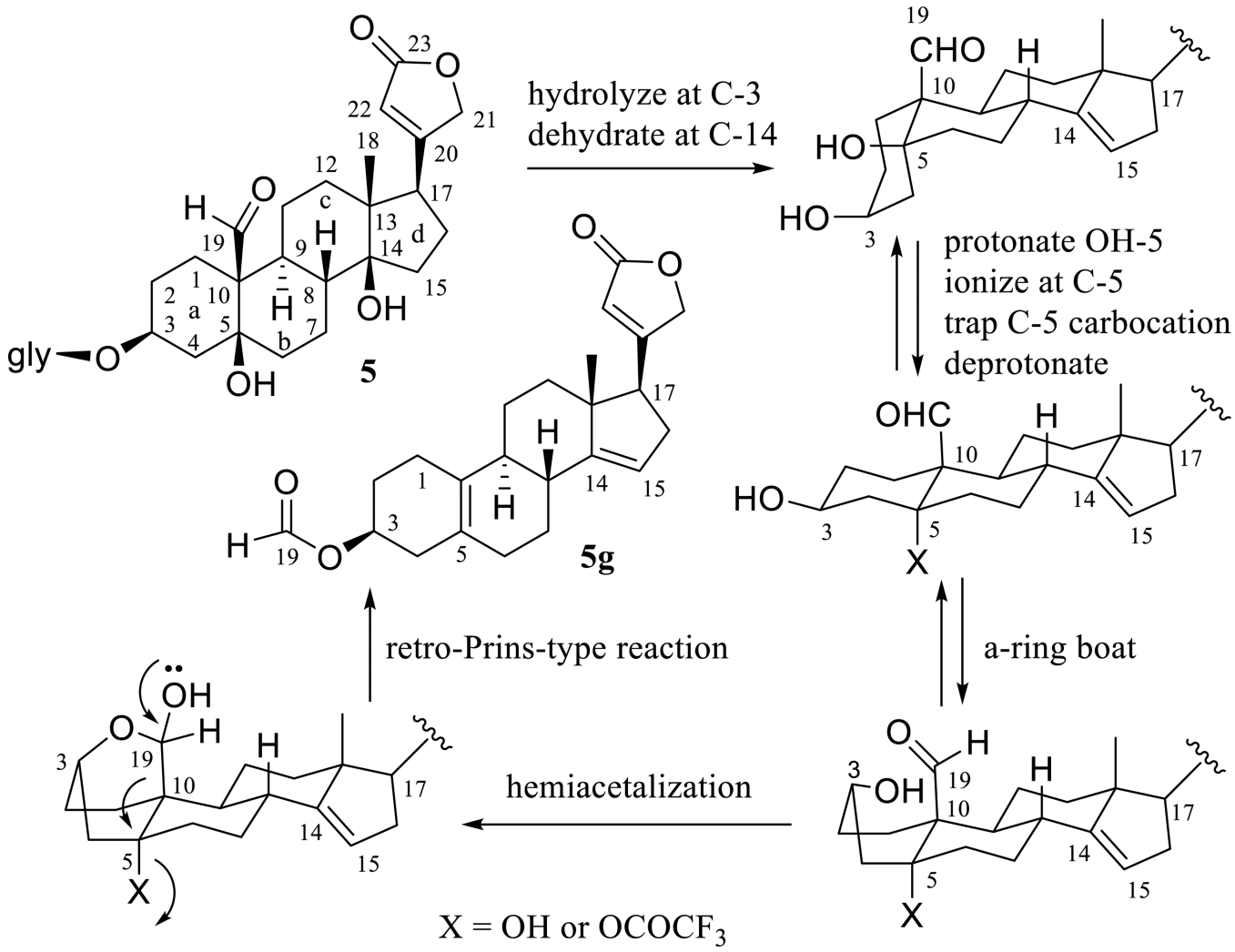

Scheme 1.
Plausible mechanism of formation of **5g** from the reaction of **5** and TFA.

Table 1

^{1}H NMR Spectroscopic Data of **1**–**3** and **5**[a]

position	1[b]	2[c]	3[d]	5[c]
1	α 1.20 m β 2.02 m	α 1.85 m β 1.80 m	α 1.73 m β 1.31 m	α 1.24 m β 2.02 m[e]
2	1.62[e] 1.94[e]	1.64 m 1.80 m	1.75 m 1.91 m	1.96 m[e] 2.02 m[e]
3	α 4.25 m	α 4.19 m	α 4.14 m	α 4.22 br s
4	1.54[e] 2.05[e]	α 1.74 m β 2.07 m	α 1.59 m β 2.17 m	1.68[e] 1.96 m[e]
6	2.02[e] 1.66[e]	1.74 m 1.44 m[e]	1.71 m 1.25	2.02 m[e] 1.68[e]
7	α 1.39 m β 2.59 dt (14.6, 3.2)	α 1.89 m β 1.17 m	α 1.98 m β 1.29	α 1.72 m β 2.23 m
8	β 1.54[e]	β 1.56[e]	β 1.52 m	β 1.90 m[e]
9	α 1.57[e]	α 1.51[e]	α 1.50 m	α 2.06 m
11	1.51[e] 1.32 m	1.48 m 1.44 m[e]	α 1.46 m β 1.33 m	1.51[e]
12	1.39[e] 1.54[e]	1.51[e] 1.56[e]	1.67[e] 1.81 m	1.38 m 1.51[e]
15	2.02[e] 1.71 m	α 2.03 m β 1.74 m	α 2.14 m β 1.77 m	1.68[e] 1.96 m[e]
16	α 2.19 m β 1.87 m	α 2.18 m β 1.89 m	α 2.11 m β 1.93 m	2.16 m 1.90 m[e]
17	α 2.79 dd (9.4, 5.4)	α 2.81 dd (9.2, 4.6)	α 2.85[e]	α 2.77 dd (8.8, 5.2)
18	β 0.86 s	β 0.88 s	β 0.91 s	β 0.86 s
19	4.33[e] 3.45 t (10.1)	β 0.96 s	β 0.92 s	β 10.02 s
21	5.00 dd (18.1, 1.4) 4.82 dd (18.1, 1.6)	5.00 d (17.2) 4.83 d (17.7)	5.03 d (17.9) 4.87 d (18.2)	4.81 d (18.0) 4.96 d (18.0)
22	5.88 br s	5.89 br s	5.87 br s	5.87 br s
1'	α 4.33[e] α 4.38 d (7.1)[f]	α 4.46 d (8.0)	α 4.73 d (7.8)	α 4.34 d (6.4)
2'	β 3.26[e] β 3.21 m[f]	β 3.03 t (9.0)	β 3.02 dd (7.8, 2.7)	β 3.23[e]
3'	α 3.25[e] α 3.23 m[f]	α 3.19 t (9.2)	α 4.26 m	α 3.21[e]
4'	α 3.82 m α 3.83 m[f]	β 3.51 m	α 3.14 m	α 3.81 br s
5'	α 3.54[e] α 3.63 m[f]	α 3.36 m	α 3.68 dd (9.2, 6.3)	α 3.51[e]
6'	β 1.35 d (6.5)	3.79 m 3.88 m	β 1.19 d (6.2)	β 1.35 d (6.4)

position	1[b]	2[c]	3[d]	5[c]
	β 1.26 d (6.5)[f]			
OH-5	β 4.76 br s	β 3.49 m	β 3.98 m	β 4.37 br s
OH-19	4.50 br d (9.1)			
OH-4'	β 2.39 br s	α 2.48 m		
OH-6'		β 1.95 m		
OCH_3-2'	α 3.56 s	α 3.61 s	α 3.38 s	α 3.55 s
OCH_3-3'	β 3.49 s	β 3.64 s		β 3.48 s

[a] Assignments of chemical shifts are based on the analysis of 1D- and 2D-NMR spectra. The overlapped signals were assigned from ^1H–^1H COSY, HSQC, and HMBC spectra without designating multiplicity.

[b] Data (δ) measured in $CDCl_3$ at 400.13 MHz and referenced to the internal standard TMS residual peak at δ 0.00.

[c] Data (δ) measured in $CDCl_3$ at 400.13 MHz and referenced to the solvent residual peak at δ 7.26.[21]

[d] Data (δ) measured in acetone-d_6 at 400.13 MHz and referenced to the internal standard TMS residual peak at δ 0.00.

[e] The overlapped signals.

[f] Data (δ) measured in acetone-d_6 at 400.13 MHz and referenced to the solvent residual peak at δ 2.05.[21]

Table 2

^{13}C NMR Spectroscopic Data of **1**–**3** and **5**[a]

position	1[b]	2[b]	3[c]	5[d]
1	24.0 CH_2	26.1 CH_2	26.4 CH_2	24.3 CH_2
2	25.6 CH_2	25.3 CH_2	26.8 CH_2	25.3 CH_2
3	73.2 CH	75.6 CH	75.2 CH	72.9 CH
4	34.9 CH_2	34.2 CH_2	34.7 CH_2	34.3 CH_2
5	77.1 C	73.0 C	73.2 C	73.2 C
6	33.8 CH_2	34.5 CH_2	36.2 CH_2	36.6 CH_2
7	19.0 CH_2	23.8 CH_2	24.6 CH_2	18.1 CH_2
8	40.4 CH	40.9 CH	41.5 CH	41.8 CH
9	39.1 CH	39.2 CH	39.6 CH	39.5 CH
10	42.4 C	40.8 C	41.6 C	54.7 C
11	21.1 CH_2	21.5 CH_2	22.4 CH_2	22.1 CH_2
12	40.1 CH_2	40.1 CH_2	40.5 CH_2	40.0 CH_2
13	49.4 C	49.4 C	50.3 C	49.6 C
14	85.4 C	85.6 C	85.5 C	85.4 C
15	32.5 CH_2	33.1 CH_2	33.5 CH_2	32.1 CH_2
16	26.8 CH_2	26.8 CH_2	27.5 CH_2	27.0 CH_2
17	50.6 CH	50.7 CH	51.6 CH	50.6 CH
18	15.7 CH_3	15.7 CH_3	16.1 CH_3	15.7 CH_3
19	65.0 CH_2	16.8 CH_3	17.2 CH_3	208.3 CH
20	174.4 C	174.4 C	176.3 C	174.3 C
21	73.5 CH_2	73.4 CH_2	73.9 CH_2	73.6 CH_2
22	117.8 CH	117.9 CH	117.8 CH	118.0 CH
23	174.5 C	174.2 C	176.4 C	174.5 C
1'	99.4 CH	101.0 CH	98.1 CH	100.0 CH
2'	80.0 CH	83.8 CH	81.6 CH	80.1 CH
3'	83.9 CH	86.2 CH	68.6 CH	84.0 CH
4'	68.4 CH	70.7 CH	73.8 CH	68.5 CH
5'	70.5 CH	75.1 CH	70.4 CH	70.5 CH
6'	16.4 CH_3	62.8 CH_2	18.3 CH_3	16.5 CH_3
OCH_3-2'	61.2 CH_3	60.9 CH_3	57.1 CH_3	61.4 CH_3
OCH_3-3'	57.6CH_3	61.0 CH_3		57.8 CH_3

[a]Assignments of chemical shifts are based on the analysis of 1D- and 2D-NMR spectra. CH_3, CH_2, CH, and C multiplicities were determined by DEPT 90, DEPT 135, and HSQC experiments.

[b]Data (δ) measured in $CDCl_3$ at 100.61 MHz and referenced to the internal standard TMS residual peak at δ 0.00.

[c]Data (δ) acetone-d_6 at 100.61 MHz and referenced to the internal standard TMS residual peak at δ 0.00.

[d]Data (δ) measured in $CDCl_3$ at 100.61 MHz and referenced to the solvent residual peak at δ 77.16.[21]

Table 3

Cytotoxicity against Human Colon and Lung Cancer and Leukemia Cell Lines of **1**–**5**[a]

compound	HT-29[b]	MV4–11[c]	Kasumi-1[d]	H1299[e]
1	160	186	181	290
2	690	NT[g]	NT[g]	NT[g]
3	360	NT[g]	NT[g]	NT[g]
4	90	99	97	NT[g]
5	170	90	86	110
digoxin	380	111	93	460
paclitaxel[f]	0.8			1500
silvestrol[f]		11	24	

[a] IC_{50} values are the concentration (nM) required for 50% inhibition of cell viability for a given test compound and were calculated using nonlinear regression analysis with measurements performed in triplicate and representative of three independent experiments, where the values generally agreed within 10%.

[b] IC_{50} value toward the HT-29 human colon cancer cell line with 72 h treatment.

[c,d] IC_{50} value toward the human MV4–11 and Kasumi-1 leukemia cell lines, respectively, with 48 h treatment.

[e] IC_{50} value toward the H1299 human non-small cell lung cancer cell line with a 24 h treatment

[f] Positive control.

[g] Not tested.

Table 4

Growth Inhibitory Activity against Normal Human Cells of **5**[a]

compound	CCD-112CoN[b]	blood cells[c]	NL20[d]
5	>20	>20	10.0
digoxin	2.4	>20	7.0

[a] IC_{50} values are the concentration (μM) required for 50% inhibition of cell viability with a given test compound and were calculated using nonlinear regression analysis with measurements performed in triplicate and representative of three independent experiments, where the values generally agreed within 10%.

[b] IC_{50} value toward normal human colon CCD-112CoN cell line with a 72 h treatment.

[c] IC_{50} value toward normal human peripheral blood mononuclear cells with a 48 h treatment.

[d] IC_{50} value toward normal human lung NL20 cell line with a 24 h treatment.

Table 5

Cytotoxicity against Human Colon Cancer Cell Line of **5** and **5a**–**5g**[a]

compound	HT-29[b]
5	0.17
5a	0.47
5b	1.2
5c	>20
5d	2.8
5e	>20
5f	>20
5g	>20
paclitaxel[c]	0.0008

[a] IC_{50} values are the concentration required for 50% inhibition of cell viability after 72 h incubation for a given test compound and were calculated using nonlinear regression analysis with measurements performed in triplicate and representative of three independent experiments, where the values generally agreed within 10%.

[b] IC_{50} value (μM) toward the HT-29 human colon cancer cell line.

[c] Positive control.

Table 6

Cytotoxicity against Human Breast and Ovarian Cancer and Melanoma Cell Lines of **5**[a]

compound	MDA-MB-231[b]	MDA-MB-435[c]	OVCAR3[d]
5	134	90	44
paclitaxel[e]	2.7	0.2	3.3

[a] IC_{50} values are the concentration (nM) required for 50% inhibition of cell viability for a given test compound with a 72 h treatment and were calculated using nonlinear regression analysis with measurements performed in triplicate and representative of three independent experiments, where the values generally agreed within 10%.

[b] IC_{50} value toward the MDA-MB-231 human breast cancer cell line.

[c] IC_{50} value toward the MDA-MB-435 human melanoma cell line.

[d] IC_{50} value toward the OVCAR3 human ovarian cancer cell line.

[e] Positive control.